OPEN ACCESS Freely available online

PLOS ONE

Docking, Synthesis and Antiproliferative Activity of *N*-Acylhydrazone Derivatives Designed as Combretastatin A4 Analogues

Daniel Nascimento do Amaral[1,2], Bruno C. Cavalcanti[3], Daniel P. Bezerra[3], Paulo Michel P. Ferreira[4], Rosane de Paula Castro[5], José Ricardo Sabino[5], Camila Maria Longo Machado[6], Roger Chammas[6], Claudia Pessoa[3], Carlos M. R. Sant'Anna[7], Eliezer J. Barreiro[1,2], Lídia Moreira Lima[1,2]*

1 Instituto Nacional de Ciência e Tecnologia de Fármacos e Medicamentos (INCT-INOFAR). Universidade Federal do Rio de Janeiro, Laboratório de Avaliação e Síntese de Substâncias Bioativas (LASSBio) Rio de Janeiro, Brasil, **2** Programa de Pós-Graduação em Química, Instituto de Química, Universidade Federal do Rio de Janeiro, Rio de Janeiro, Brasil, **3** Departamento de Fisiologia e Farmacologia, Faculdade de Medicina, Universidade Federal do Ceará, Fortaleza, Brasil, **4** Departamento de Ciências Biológicas, Campus Senador Helvídio Nunes de Barros, Universidade Federal do Piauí, Picos, Brasil, **5** Instituto de Física, Universidade Federal de Goiás, Goiânia, Brazil, **6** Faculdade de Medicina, Departamento de Radiologia, Universidade de São Paulo, São Paulo, Brasil, **7** Departamento de Química, Universidade Federal Rural do Rio de Janeiro, Seropédica, Brasil

Abstract

Cancer is the second most common cause of death in the USA. Among the known classes of anticancer agents, the microtubule-targeted antimitotic drugs are considered to be one of the most important. They are usually classified into microtubule-destabilizing (e.g., Vinca alkaloids) and microtubule-stabilizing (e.g., paclitaxel) agents. Combretastatin A4 (CA-4), which is a natural stilbene isolated from *Combretum caffrum*, is a microtubule-destabilizing agent that binds to the colchicine domain on β-tubulin and exhibits a lower toxicity profile than paclitaxel or the Vinca alkaloids. In this paper, we describe the docking study, synthesis, antiproliferative activity and selectivity index of the *N*-acylhydrazone derivatives (**5a–r**) designed as CA-4 analogues. The essential structural requirements for molecular recognition by the colchicine binding site of β-tubulin were recognized, and several compounds with moderate to high antiproliferative potency (IC_{50} values $\leq$ 18 μM and $\geq$4 nM) were identified. Among these active compounds, LASSBio-1586 (**5b**) emerged as a simple antitumor drug candidate, which is capable of inhibiting microtubule polymerization and possesses a broad *in vitro* and *in vivo* antiproliferative profile, as well as a better selectivity index than the prototype CA-4, indicating improved selective cytotoxicity toward cancer cells.

Citation: do Amaral DN, Cavalcanti BC, Bezerra DP, Ferreira PMP, Castro RdP, et al. (2014) Docking, Synthesis and Antiproliferative Activity of *N*-Acylhydrazone Derivatives Designed as Combretastatin A4 Analogues. PLoS ONE 9(3): e85380. doi:10.1371/journal.pone.0085380

Editor: Kamyar Afarinkia, Univ of Bradford, United Kingdom

Received September 4, 2013; **Accepted** November 26, 2013; **Published** March 10, 2014

Funding: This work was supported by CNPq (BR), FAPERJ (BR) and INCT-INOFAR (BR, 573.564/2008-6 and E-26/170.020/2008). The funders had no role in study design, data collection and analysis, decision to publish, or preparation of the manuscript.

Competing Interests: The authors have declared that no competing interests exist.

* E-mail: lidia@lassbio.icb.ufrj.br

Introduction

Microtubules (MTs) are cytoskeletal polymers formed by the polymerization of á- and β-tubulin heterodimers, which is followed by GTP hydrolysis; the polymerization occurs through two important steps: nucleation and elongation. MTs are found within all dividing eukaryotic cells, as well as in most differentiated cell types, and play crucial roles in cell division, cell motility, cellular transport, the maintenance of cell polarity, and cell signaling [1].

Microtubules are labile polymers that display two types of dynamic behaviors, which are called "treadmilling" and "dynamic" instability. The latter, is characterized by the alternating growing and shortening phases of the microtubule ends. The transition from a growing phase to a shortening phase is called a catastrophe, while a transition from a shortening phase to a growing phase is known as a rescue. Because microtubule dynamics play an important role in various cellular functions, such as mitosis, they are a potential target for development of anticancer drugs [1–4].

Microtubule-targeting antimitotic drugs are usually classified into two main groups. One group, which is composed of microtubule-destabilizing agents, inhibits microtubule polymerization and includes compounds such as the Vinca alkaloids, vincristine (**1**) and vinblastine (**2**) (Figure 1); these two compounds were the first anti-microtubule agents approved to treat cancer. The second group encompasses the microtubule-stabilizing agents; these compounds stimulate microtubule polymerization and include paclitaxel, which is used to treat breast and ovarian cancer, non-small-cell lung cancer and Kaposi's sarcoma [4].

While vinblastine binds close to the exchangeable GTP site on the β-tubulin in a region called the Vinca-binding domain, paclitaxel (**3**, Figure 1) binds to the inner surface of the microtubules in a deep hydrophobic pocket on the βtubulin; this site is called the paclitaxel binding site [4–5].

During the development of orally bioavailable anti-microtubule agents that overcome the neurotoxicity and development of resistance commonly observed with the Vinca alkaloids, paclitaxel and their analogues, combretastatin A4 (CA-4, Figure 1) was

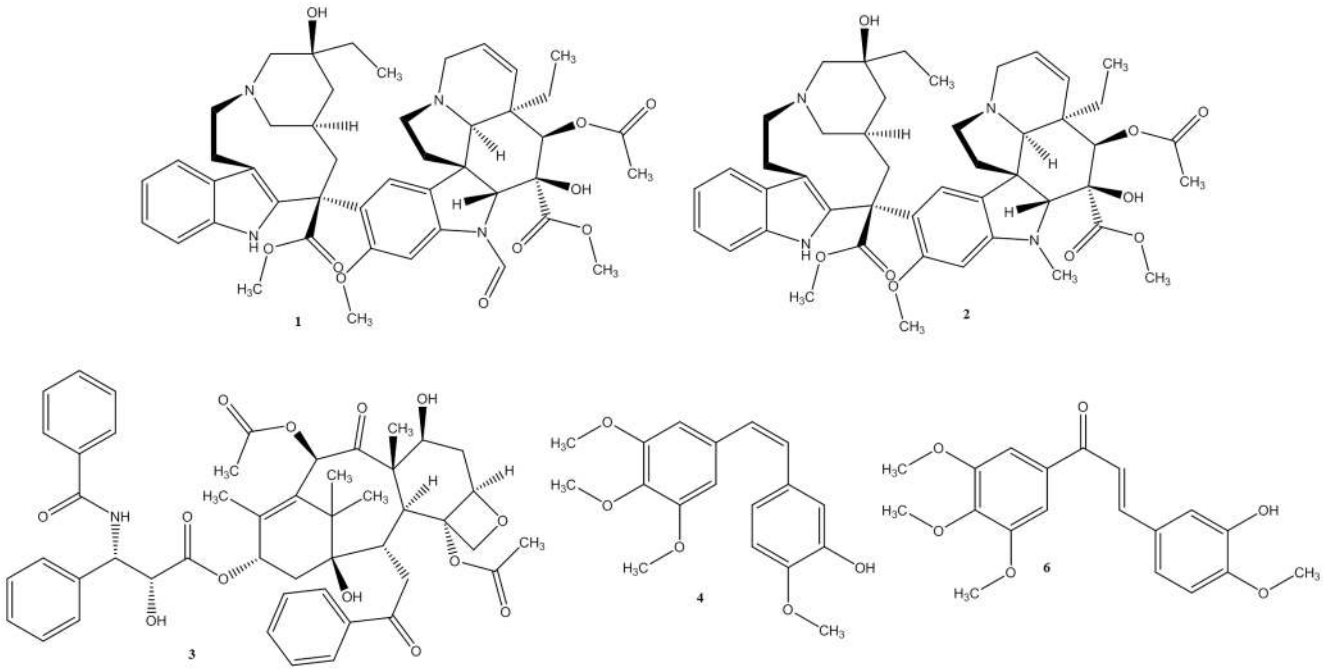

Figure 1. Anti-microtubule agents: vincristine (1), vinblastine (2), paclitaxel (3), CA-4(4) and its chalcone analogue (6).
doi:10.1371/journal.pone.0085380.g001

discovered and is currently considered a promising lead-compound. This stilbene natural product, which was isolated from *Combretum caffrum*, binds to the colchicine domain on β-tubulin and exhibits a low toxicity profile [6]. Despite its potent antiproliferative activity, CA-4 (**4**) failed to exhibit anticancer efficacy in animal models because it has low water solubility, poor oral bioavailability, a short half-life and a double bond that isomerizes (*Z* to *E*) in vivo; this isomerization causes a loss of affinity for β-tubulin and consequently a loss of cytotoxic activity [7–11].

This paper describes the docking studies, synthesis and assessment of antiproliferative activity and selectivity index of *N*-acylhydrazone derivatives (**5a–r**) designed as CA-4 analogues.

The initial design conception of the *N*-acylhydrazone derivatives (**5a–r**) is depicted in Figure 2. The most important structural modification was the replacement of ethylene linker between the aromatic subunits **A** and **B** with a more stable *N*-acylhydrazone (NAH) scaffold, generating compound **5a**. To design a congeneric series (**5b–r**), several modifications were introduced in the substitution of aromatic subunit **B** based on docking studies with the colchicine binding site of the β-tubulin protein.

Results and Discussion

All designed compounds were predicted to favorably interact with the DAMA-colchicine binding site in β-tubulin (PDB code: 1sa0) [12]. In the best-ranked solutions, there were few polar interactions, and the complementarity between the ligand and the receptor protein involved extensive, nonspecific interactions with hydrophobic groups. These results were in accordance with the DAMA-colchicine interaction mode observed in the co-crystallized structure: there is only one polar interaction, which occurred between the Cys241 SH group and one of the methoxy groups on the ligand (data not shown). Previously, the proximity between these groups was explored to establish a cross-link between the colchicine derivatives substituted at this methoxy position and Cys241 [13]. Combretastatin A4 (CA-4) was also predicted to interact primarily with the hydrophobic groups; its trimethoxy ring (ring **A**) occupied a similar position to the corresponding colchicine ring, and its second ring (ring **B**) formed two hydrogen bonds, which were between its phenolic hydroxyl group and Thr179 peptide carbonyl group, as well as between the adjacent methoxy group and Ser178 side chain [7,10,11]. Similar studies performed with the *E*-isomer CA4 show the loss of interactions with residues Ser178 and Thr179, which may somehow explain the inactivity of this isomer (see Figure S2 in supporting material). Additionally, its *N*-acylhydrazone analogue, which was LASSBio-1593 (**5a**), interacted with Ser178 through a methoxy group on ring **A**, and its isovaline ring (ring **B**) formed two hydrogen bonds, one with Val238 and the other with Tyr202 (Figure 3).

Based on the docking studies with compound **5a**, several modifications were enacted on the 4-methoxy-3-hydroxy-phenyl moiety (ring **B**, Figure 2) to vary the oxygenated pattern (**5c–j**) and explore more lipophilic substituents (**5b**, **5l–r**), while making allowances for the hydrophobic nature of colchicine binding pocket (Table 1). The modification of the linker between rings **A** (*i.e.*, 3,4,5-trimethoxyphenyl) and **B** (*i.e.*, 3-hydroxy,4-methoxy-phenyl) resulted in the introduction of an *N*-acylhydrazone (NAH) subunit to replace the ethylene bridge (CH = CH). As expected, this type of modification caused significant conformational changes and altered the spatial arrangement of rings **A** and **B** during molecular recognition by β-tubulin (Figure 2). These findings are supported by data from the literature describing the anti-tubulin activity of *E*-chalcones (e.g., **6**, Figure 1) [14–16]. Additionally, the introduction of halogens substituents at position 4 of the **B** ring took advantage of the metabolic protection that might be exerted by these substituents, preventing aromatic hydroxylation at C4 catalyzed by the CYP450 enzymatic complex [17].

To identify the most energetically favorable pose (*i.e.*, pose prediction), each pose of the *N*-acylhydrazone derivatives **5a–r** within the colchicine binding site of β-tubulin was evaluated (*i.e.*, scored) based on their complementarity to the target with respect

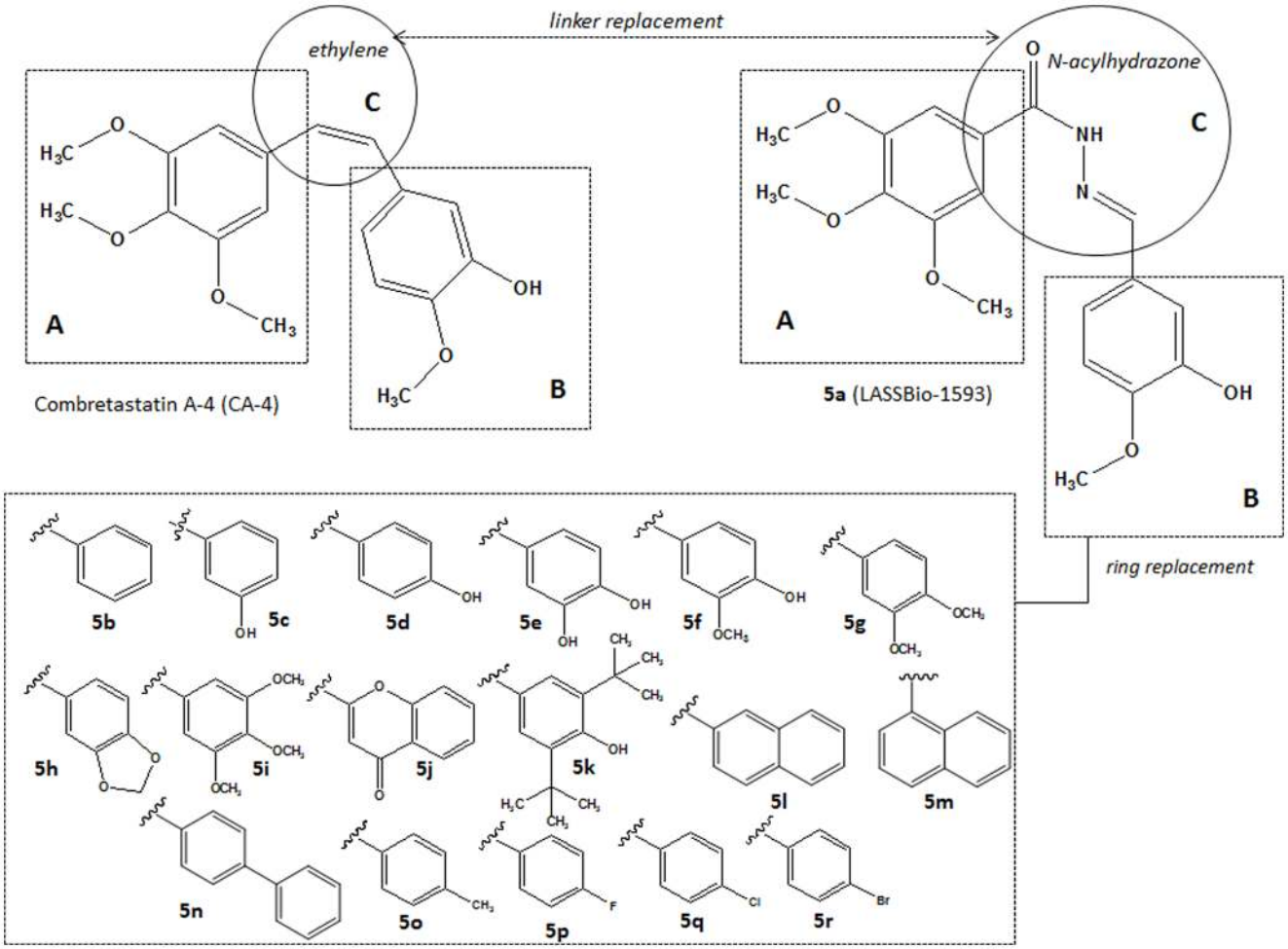

Figure 2. Initial conception and molecular design of *N*-acylhydrazone derivatives 5a–s.
doi:10.1371/journal.pone.0085380.g002

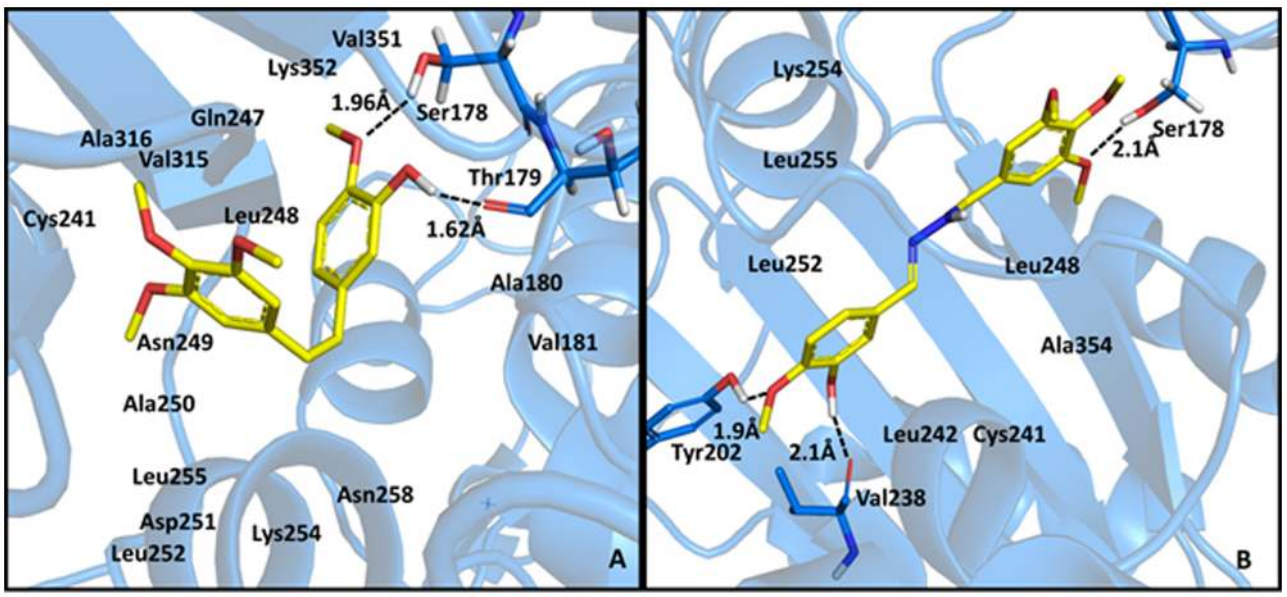

Figure 3. Polar interactions between CA-4 (A) or LASSBio-1593 (B) with the colchicine binding site of β-tubulin (PDB code: 1sa0).
doi:10.1371/journal.pone.0085380.g003

Table 1. Scores estimated by molecular docking (ChemScore fitness function) for colchicine binding site of β-tubulin, cLogP, $cLogD_{7.0}$, molar refractivity and the aqueous solubility of CA-4 and its *N*-acylhydrazone analogues **5a–r**.

Compounds	Score[1] (S.D.)	cLogP[2]	cLogD[2]	MR (S.D.)[3]	Aq. Solubility (mg/mL)[4]
5a	24.64 (0.76)	2.76	2.29	93.03 (0.5)	2.84×10^{-2}
5b	24.54 (1.10)	3.15	2.78	86.36 (0.5)	3.95×10^{-2}
5c	24.43 (0.33)	2.73	2.62	87.21 (0.5)	5.68×10^{-3}
5d	35.26 (0.94)	2.72	2.64	87.21(0.5)	1.5×10^{-2}
5e	25.29 (0.44)	2.56	2.51	88.07 (0.5)	3.94×10^{-3}
5f	24.47 (0.53)	2.76	2.71	93.03 (0.5)	1.35×10^{-3}
5g	23.35 (0.63)	2.95	2.17	97.99 (0.5)	1.94×10^{-3}
5h	22.76 (0.36)	3.02	2.24	91.2 (0.5)	1.34×10^{-3}
5i	22.54 (0.64)	2.82	2.23	103.8 (0.5)	8.94×10^{-5}
5j	24.21 (0.57)	6.11	5.55	99.88 (0.5)	7.83×10^{-4}
5k	27.96 (0.84)	4.37	3.04	124.04 (0.5)	2.36×10^{-5}
5l	29.19 (0.35)	4.33	3.96	102.25 (0.5)	4.89×10^{-4}
5m	29.21 (0.91)	4.37	3.86	102.25 (0.5)	6.90×10^{-5}
5n	30.66 (1.29)	5.00	4.50	111.47 (0.5)	6.06×10^{-5}
5o	26.23 (0.99)	3.60	3.05	90.79 (0.5)	6.93×10^{-3}
5p	22.98 (1.21)	3.34	3.02	86.23 (0.5)	2.09×10^{-2}
5q	24.90 (0.73)	3.89	3.69	90.96 (0.5)	2.84×10^{-2}
5r	25.08 (0.66)	4.11	3.69	93.92 (0.5)	2.62×10^{-4}
CA-4	26.45 (1.53)	3.47	2.50	92.24 (0.3)	5.44×10^{-3}

[1]Values shown are the mean of 5 runs;
[2]cLogP and cLogD (pH 7.0) were calculated using MetaSite Program (license number: URJ181011);
[3]molar refractivity (MR) calculated with ChemSketch 12.0 (Freeware Version);
[4]Solubility was determined by ultraviolet spectroscopy, as described by Schneider and co-workers.
doi:10.1371/journal.pone.0085380.t001

to their shape and properties, such as electrostatics. It is noteworthy that score is the most adequate way of selecting the best pose, since the scores are assigned according to the interaction mode of a ligand with the binding site, as measured by fitness function. The fitness function was selected after redocking experiments with colchicine in the binding site of β-tubulin (PDB code: 1sa0). The RMSD between the experimental structure and the top scored pose, determined after redocking experiments with the four fitness functions available in GOLD 5.0.1 program (*i.e.* Chemscore, Goldscore, ASP and ChemPLP), revealed that Chemscore was the fitness function with the best performance in this study (RMSD = 1.0606).

Giving a good score to a compound indicates that it exhibited good binding with the protein, and the results were compared to the data obtained with CA4 (Table 1). As depicted in Table 1, five compounds (**5d**, **5k**, **5l**, **5m** and **5n**) were predicted to display better binding than CA4. In this group, the most favorable complementary interaction was observed with compound **5d** (LASSBio-1588), which forms a hydrogen bond between the hydroxyl group on ring B (*i.e.*, 4-hydroxyphenyl) with Val 662. However, compounds **5k**, **5l**, **5m** and **5n** display complementary interactions using the lipophilic nature of ring B to exploit the hydrophobic pocket composed by residues Leu242, Val238, and Leu255 at the colchicine site of β-tubulin (data not shown). These data agree with the work of Dorléans and coworkers: ligands of the colchicine binding site establish few polar interactions within the protein-ligand complex, and van der Waals interactions are more relevant during molecular recognition [18]. The worst scores were observed with compounds **5g**, **5h**, **5i** and **5p**, which possessed polar groups on ring **B** that could not act as hydrogen bond donors. The score values determined during the docking studies and some physicochemical properties (cLogP, cLogD, MR and the aqueous solubility) for compounds **5a–r** are summarized in Table 1 (see also Figure S3 in supporting material).

The *N*-acylhydrazones (**5a–r**) were obtained at a two-step linear route (Figure 4) [19], using methyl 3,4,5-trimethoxybenzoate ester (**7**) as the starting material. While exploring a hydrazinolysis reaction, ester **7** was refluxed with hydrazine hydrate 80% in ethanol, providing the 3,4,5-trimetoxybenzohydrazide (**8**) in 93% yield. The hydrazide (**8**) was condensed with the appropriate aldehydes, which were selected in accordance with the molecular design depicted in Figure 1, in the presence of ethanol and catalytic hydrochloric acid to furnish the CA-4 analogues **5a–r** in high yields.

Compounds **5a–r** were characterized by ^{1}H NMR, ^{13}C NMR and IR spectroscopy and their purity was determined by HPLC, with a reverse-phase column at different systems of mobile phase. All *N*-acylhydrazone derivatives (**5a–r**) were obtained as a single diastereoisomer (*Z* or *E*), as indicated by the analysis of the ^{1}H and ^{13}C NMR spectra; no duplicate signals attributed to the hydrogen or carbon atom of the imine (N = CH) were observed. The stereochemistry of the imine double bond was subsequently assigned based on our previous results [23] and the X-ray crystallographic studies performed with **5b** (LASSBio-1586).

A single crystal of compound **5b** (LASSBio-1586) was obtained and subjected to X-ray diffraction; the ORTEP [20,37] view is shown in Figure 5. Crystallographic analysis confirmed that the configuration about the C2 = N2 double bond [distance 1.273(3) Å] was *E* and revealed a nearly flat conformation of the benzoylhydrazide moiety, which was described by the least

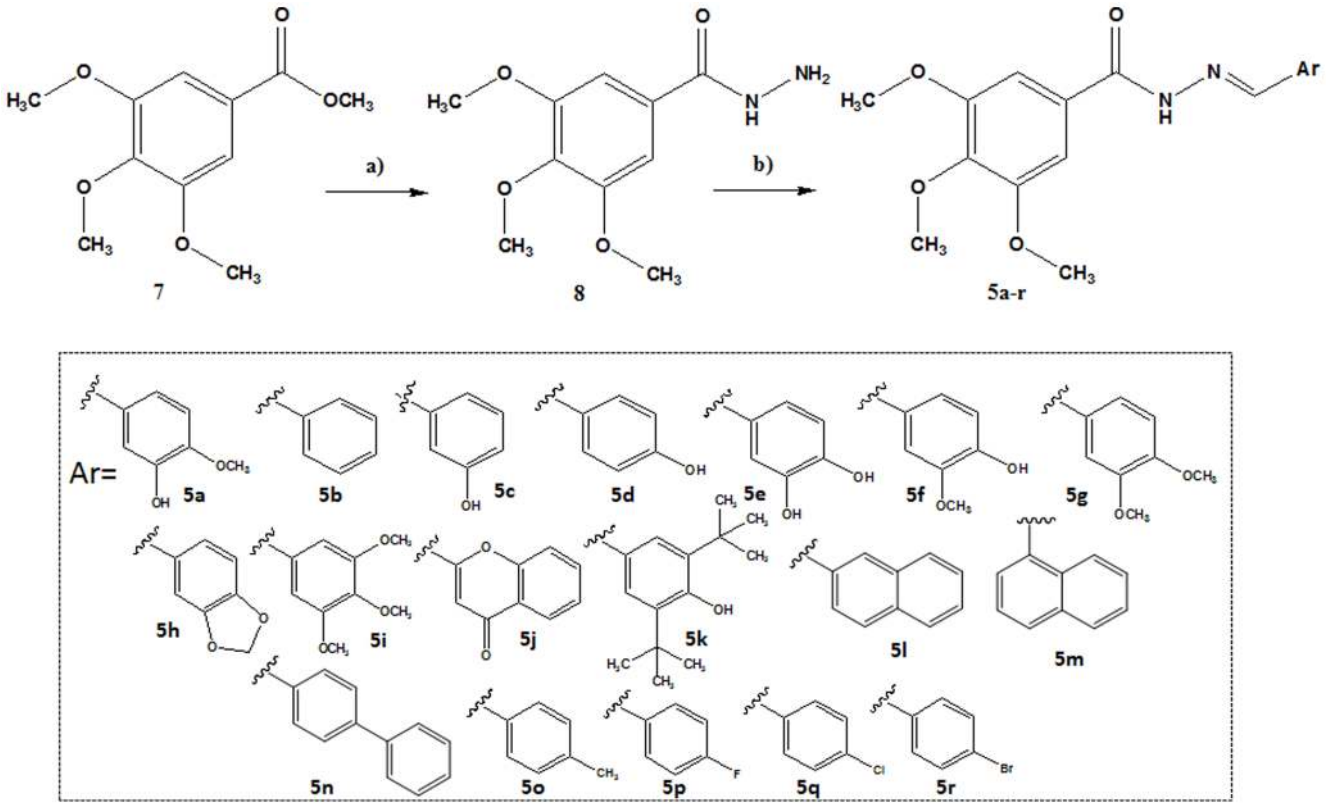

Figure 4. Conditions and reagents: a) 80% aq. $N_2H_4.H_2O$, EtOH, reflux, 2 h, 93%. b) ArCHO, EtOH, HCl (cat), r.t., 0.5–4 h, 62–95%.
doi:10.1371/journal.pone.0085380.g004

squares plane through the atoms O1/N1/C1/N2/C2/C9/C10/C11/C12/C13/C14 with a r.m.s. deviation of 0.066 Å, as well as C2—C9 bond torsion angles of 3.4 (3)° and −174.9 (2)°, respectively. The trimethoxyphenyl ring was rotated outward from this plane by 45.31(6)°, reducing the π-orbital contribution to this bond and allowing an elongation of the C1—C3 bond [1.499 (3) Å] relative to the expected bond length. One feature of acentric crystal structures occurs in this case, which is that torsional angles of the methoxy groups are unique, as given by: C4—C5—O2—C15 of 5.1 (3)°, C7—C6—O3—C16 of −56.0 (3)° and C8—C7—O4—C17 of 13.9 (3)°. The molecules are connected through an N—H…O intermolecular hydrogen bond with the carbonyl group and are arranged in a linear array though crystal axis a. The parallel arrays are bound by weak van der Waals interactions between methyl group C15 and the O2 oxygen atom from a neighboring molecule, demonstrating the availability of this group for intermolecular interactions once the methoxy group in the *para* position is rotated to the opposite side. Crystallographic data of compound **5b** (excluding structure factors) can be seen in supporting information. Crystallographic data of compound **5b** (excluding structure factors) can be seen in supporting information.

The antiproliferative activity of compounds **5a–r** was determined based on an MTT assay [21] and using CA-4 as standard against the tumor cell lines: HL-60 (human leukemia), SF-295 (human glioblastoma), MDA-MB435 (melanoma), PC3M (prostate cancer), OVCAR-8 (ovaries adenocarcinoma), NCI-H258M (pulmonary bronchio-alveolar carcinoma) and HCT-8 (adenocarcinoma ileocecal) (Table 2). To determine the selectivity index of compounds **5a–r**, their antiproliferative profile was also evaluated toward human lymphocytes (Table 2).

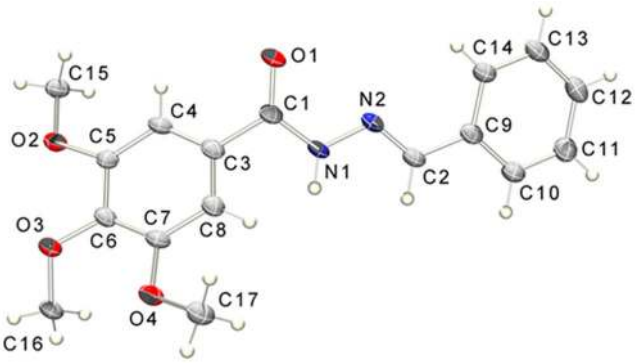

Figure 5. ORTEP view of compound 5b with the atom displacement ellipsoids drawn at a 50% probability level.
doi:10.1371/journal.pone.0085380.g005

As shown in Table 2, all compounds except for derivatives **5i**, **5j**, **5k** and **5n** exhibited moderate to high antiproliferative potency with IC_{50} values ≤18 μM and ≥4 nM. These results are in agreement with Jin and co-workers [22], who described the antiproliferative activity of some NAH containing the trimethoxyphenyl subunit against PC3, A431 and BGC823 tumor cells for the first time. The *N*-acylhydrazones with hydrophobic substituents on ring B (*i.e.*, **5l**, **5m**, **5o**, **5p**, **5q** and **5r**) were more potent, which was predicted by the score values obtained from the docking studies. The *in silico* study failed to predict the cytotoxic activity of compound **5n** and **5d**, which scored as better binders than CA-4. The inactivity of compound **5n** (IC_{50}>25 μM) suggested that there were steric constraints in the recognition between the ligand

Table 2. *In vitro* antiproliferative potency (IC_{50}-μM) of compounds **5a–r** and the standard CA-4 against tumor cell lines and human lymphocytes.

Compounds	*HL-60*	*SF295*	*HCT-8*	*MDA-MB435*	*PC3M*	*OVCAR-8*	*NCI-H358M*	*Lymphocytes*
5a	4.72	1.55	2.08	0.39	2.22	1.44	1.58	2.58
5b	0.29	0.26	0.45	0.064	0.8	0.29	0.35	1.34
5c	1.63	13.05	4.3	0.12	7.51	5.78	9.5	4.48
5d	2.63	15.95	6.54	0.88	4.57	6.18	11.75	13.38
5e	9.3	>25	>25	11.78	24.4	>25	>25	7.36
5f	9.85	13.57	9.27	6.52	16.96	14.6	11.85	36.51
5g	4.43	18.08	7.05	2.11	12.55	7.11	10.18	17.98
5h	3.07	0.86	55.81	0.11	1.14	1.09	2.15	1.31
5i	>25	>25	>25	>25	>25	>25	>25	>61.82
5j	>25	>25	23.35	>25	>25	>25	>25	>65.38
5k	>25	>25	>25	>25	>25	>25	>25	>56.49
5l	0.015	0.057	0.011	0.004	0.008	0.0054	0.079	0.010
5m	0.018	0.085	0.050	0.043	0.027	0.026	0.63	0.010
5n	>25	>25	>25	>25	>25	>25	>25	>64.07
5o	0.0048	0.093	0.046	0.035	0.0127	0.0082	0.891	0.0073
5p	1.27	2.69	2.02	1.58	4.48	0.96	2.16	3.82
5q	0.036	0.072	0.046	0.018	0.0275	0.024	1.055	0.060
5r	0.0109	0.059	0.022	0.0183	0.0127	0.0073	0.167	0.0314
CA-4	0.0021	0.0062	0.0053	0.0079	0.0047	0.00037	0.008	0.0032

doi:10.1371/journal.pone.0085380.t002

and the active site of β-tubulin because compounds with bulkier groups (for MR values see Table 1) attached to the imine (*i.e.***5i**, **5j, 5k** and **5n**) displayed the worst activities. Moreover, compounds **5i**, **5k** and **5n** bind differently from CA4 and **5b** at the colchicine binding site, with no interaction with residues Ser178 and/or Thr 179 (see Figure S4 in supporting material). The addition of a 2-chromone subunit caused the loss of antiproliferative potency, while the inclusion of oxygenated substituents at the phenyl ring (ring B; **5a**, **5c**, **5d**, **5e**, **5f**, **5g**, **5h**) did not significantly interfere with the cytotoxic potency compared to compound **5b**; however, these compounds were still significantly less active than CA-4 (Table 2).

To investigate the selective cytotoxic activity of the *N*-acylhydrazones derivatives (**5a–r**), their antiproliferative potency was also assessed toward human lymphocytes and the results were compared to the data from CA-4 (Table 3). The selectivity index (SI), which was the IC_{50} for human lymphocytes/IC_{50} for cancer cell lines after treatment with CA-4 and *N*-acylhydrazones (**5a–r**), was calculated, as depicted in Table 3. Excluding the compounds that were inactive or slightly cytotoxic (**5i**, **5j**, **5k** and **5n**), the more lipophilic (cLogP $\geq$3.15 $\leq$4.37, Table 1) compounds (**5b**, **5l**, **5m**, **5o**, **5p**, **5q**, **5r**) exhibited cytotoxic potency against human lymphocytes similar to the lead compound, CA-4. Notably, CA-4 was proven to be a non-selective cytotoxic agent, with higher antiproliferative potency against human lymphocytes versus tumor cell lines, except for HL-60 and OVCAR-8 (Table 3). In contrast, LASSBio-1586 (**5b**) exhibited a cytotoxic selectivity index from 2.4 to 42 times greater than CA-4 (Table 3; SI values for **5e** versus SI values for CA-4). The best comparative selectivity indices (CA-4 vs **5b**) were obtained from the SF-295 (SI = 13), MDA-MB435 (SI = 42) and NCI-H258M (SI = 9.5) tumor cell lines, and the worst results were found for OVCAR-8 (SI = 0.5).

Considering the IC_{50} ($\leq$0.8 μM and $\geq$0.064 μM, Table 2) and the SI values (Table 3), LASSBio-1586 (**5b**) was selected as the most promising compound, and its ability to inhibit tubulin polymerization was investigated. The tubulin polymerization assay was performed by CEREP® employing a single concentration of **5b** (C = 30 μM), using vinblastine as positive control. In this assay, LASSBio-1586 (**5b**) inhibited 91% of the tubulin polymerization, validating the rational design employed in the molecular design of the derivatives **5a–r** (data not shown; available in the supplementary information, Figure S1).

To establish the minimum structural requirements essential for the anti-tubulin activity of LASSBio-1586 (**5b**), some molecular modifications were introduced to its structure, leading to the design of compounds **9–12** (Figure 6). The *N*-acylhydrazone derivatives **9** and **10** were synthesized using the same methodology employed to obtain compounds **5a–r** [19]. The homologous compound **11** was prepared in good yield via chemoselective alkylation of the sp^3 nitrogen in the *N*-acylhydrazone functionality using methyl iodide and potassium carbonate in acetone [23]. Semicarbazone **12** was synthesized in three linear steps in 25% overall yield, as illustrated in Figure 7 [24].

The *in vitro* antiproliferative activity of compounds **9–12** was assessed against HL-60, SF296, HCT-8 and MDA-MB435 tumor cells and compared with the data from LASSBio-1586 (**5b**) and CA-4 (Table 4). As displayed in Table 4, the elimination of the methoxy groups from the trimethoxyphenyl subunit (ring A) present in LASSBio-1586 (**5b**) caused the loss of cytotoxic activity, as depicted by compound **9**, suggesting that this subunit was a pharmacophore. Similarly, retroisostere **10** was inactive, validating the role of the trimethoxyphenyl moiety as a pharmacophore when linked to the carbonyl group of the NAH functionality. The homologous compound **11** was well tolerated, exhibiting a slight increase in cytotoxic potency against HL-60 and HCT-8 tumor cell lines relative to compound **5b**. However, the aza-homologous **12** was inactive, suggesting that the semicarbazone unit was not suitable to replace the ethylene linker in CA4 or the NAH in **5b**. The greater conformational freedom introduced by the NH group may have compromised the bioactive conformation, altering the optimal spatial positioning between the aromatic rings necessary for molecular recognition with the β-tubulin binding site. To support these hypotheses, compounds **9–12** were subjected to docking studies and the best poses with the colchicine binding site of β-tubulin were analyzed (Figure 8). As presented in Figure 8, compounds **9** and **10** lost the hydrogen bond with Ser178 observed during the molecular interaction between compound **5b** and the colchicine binding pocket of β-tubulin protein. Similarly, semicarbazone **12** does not interact electrostatically with Ser178 and adopts a specific and unfavorable orientation within the active site of β-tubulin.

Considering the overall cytotoxic profile of LASSBio-1586 (**5b**) and its confirmed ability to inhibit microtubule polymerization, the antitumor activity was evaluated. The Hollow Fiber Assay (HFA) was selected because it is employed by the National Cancer Institute (NCI) as the standard model for the evaluation of new antiproliferative drugs before assessment via the *in vivo*-grown human tumor xenograft screen [25–28].

During the HFA, tumor cells (*i.e.*, SF-295 and HCT-116) were cultivated within biocompatible, semipermeable polyvinylidene fluoride hollow fibers (HFs) and subcutaneously (s.c.) implanted within the dorsal portion of BALB/c nude mice. LASSBio-1586 (**5b**) and 5-Fluorouracil (5-FU), which was the positive control, were administered intraperitoneally for 4 consecutive days. On day 5, the fibers were removed to quantify the antiproliferative activity of **5b** and 5-FU.

The hollow fibers were well tolerated by the animals, and no signs of rejection were detected. The treatments with LASSBio-1586 (**5b**) and 5-FU did not affect the health of the mice beyond acceptable limits and no deaths occurred.

As shown in Table 5, LASSBio-1586 (**5b**; dosages = 25 and 50 mg/kg/day) reduced the proliferation of both SF-295 (61.89 and 82.89%) and HCT-116 (72.68 and 80.76%) cell lines after 4 days of administration ($P<0.05$), demonstrating its antiproliferative effect *in vivo*.

Conclusions

Based on the results of docking studies, a series of *N*-acylhydrazone derivatives were used as structural analogues of CA-4. These studies identified the major structural requirements essential for molecular recognition by the colchicine binding site of β-tubulin. Of the active compounds, LASSBio-1586 (**5b**) emerged as a simple antitumor drug candidate and was capable of inhibiting microtubule polymerization; this compound also possessed broad *in vitro* and *in vivo* antiproliferative profile and a better selectivity index than the lead compound, CA-4, which indicated that **5b** displayed improved selective cytotoxicity toward cancer cells.

Methods

Ethics Statement

Procedures are in accordance with guidelines for the welfare of animals in experimental neoplasia [40] and with national and international standard on the care and use of experimental laboratory animals [41] and were approved by the local Ethical

Table 3. The selectivity index (SI) of CA-4 and *N*-acylhydrazones (**5a–r**).

Compounds	SI	SI	SI	SI	SI	SI	SI
	Lymphocyte/	Lymphocyte/	Lymphocyte/	Lymphocyte/	Lymphocyte/	Lymphocyte/	Lymphocyte/
	HL-60	SF-295	HCT-8	MDA-MB345	PC3M	OVCAR-8	NCI-H358M
CA-4	1.44±0.05	0.44±0.04	0.59±0.01	0.42±0.02	0.72 v 0.02	0.030±0.70	0.52±0.12
5a	0.56±0.01	1.89±0.19	1.31±0.11	6.30±0.30	1.40±0.30	1.65±0.15	1.70±0.10
5b	4.11±0.39	4.88±0.42	2.86±0.13	20.07±0.93	1.60±0.10	4.39±0.21	4.05±0.25
5c	2.60±0.10	0.32±0.02	0.96±0.35	32.50±4.50	0.58±0.01	0.80±0.005	0.48±0.01
5d	5.15±0.05	0.82±0.02	2.07±0.07	16.06±0.86	2.96±0.86	2.22±0.02	1.16±0.06
5e	0.82±0.02	0.02±0.00	0.02±0.00	0.06±0.00	0.30±0.005	0.2±0.00	0.30±0.00
5f	3.77±0.07	2.75±0.05	3.91±0.10	5.52±0.08	2.25±0.05	2.53±0.03	3.12±0.02
5g	4.10±0.10	0.99±0.005	2.50±0.005	8.41±0.09	1.44±0.04	2.55±0.05	1.80±0.005
5h	0.43±0.01	1.47±0.02	0.02±0.002	13.17±1.37	1.14±0.06	1.16±0.04	0.62±0.02
5i	1	1	1	1	1	1	1
5j	1	1	2.8	1	1	1	1
5k	1.1	1	1	1	1	1	1
5l	0.61±0.09	0.18±0.02	0.80±0.09	1.96±0.53	1.15±0.15	1.95±0.05	0.11±0.01
5m	0.52±0.07	0.11±0.01	0.21±0.01	0.26±0.06	0.37±0.03	0.42±0.02	0.01±0.005
5n	1.0	1.0	1.0	1.0	1	1	1
5o	1.59±0.09	0.08±0.00	0.15±0.005	0.21±0.01	0.56±0.04	0.91±0.01	0.009±0.001
5p	3.11±0.11	1.46±0.06	1.85±0.04	2.34±0.06	0.89±0.01	4.38±0.38	1.76±0.04
5q	1.85±0.15	0.85±0.05	1.25±0.05	3.07±0.22	2.10±0.10	2.75±0.25	0.05±0.005
5r	3.07±0.83	0.49±0.05	1.57±0.17	1.81 0.11	2.29±0.20	4.02±0.28	0.19±0.01

doi:10.1371/journal.pone.0085380.t003

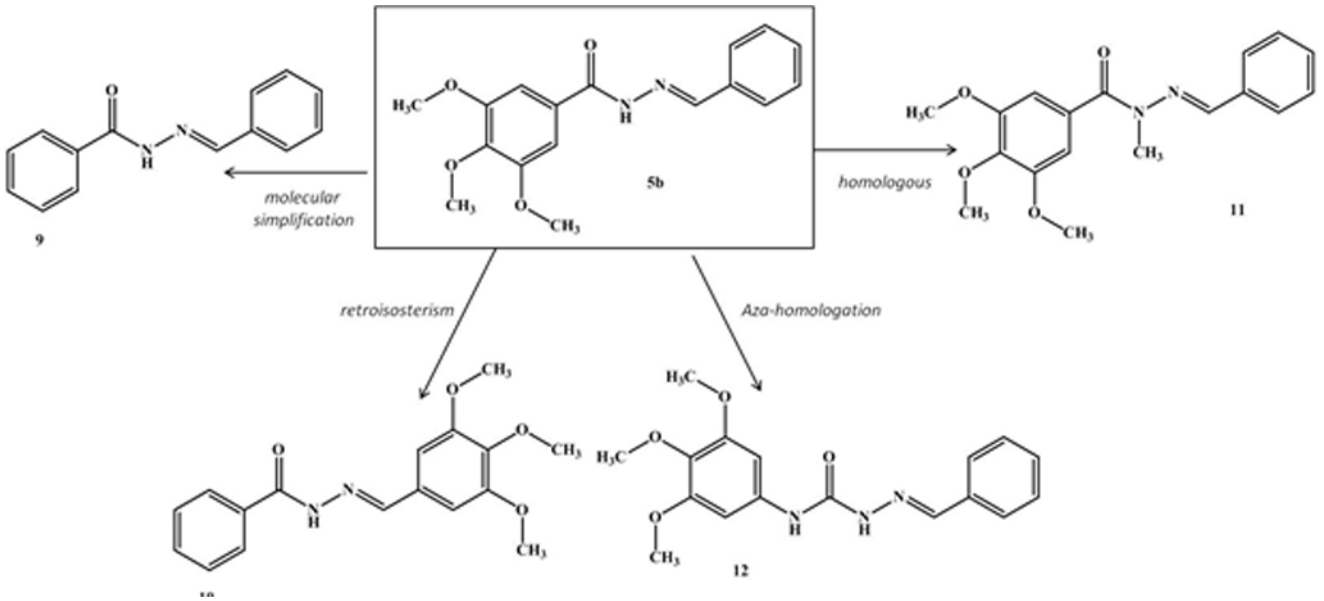

Figure 6. Design of compounds 9–12 from molecular modification of prototype 5b.
doi:10.1371/journal.pone.0085380.g006

Committee on Animal Research (Process No. 102/2007) at Federal University of Ceará (Fortaleza, Ceará, Brazil).

Chemistry

Reagents and solvents were purchased from commercial suppliers and used as received. The reactions were monitored by thin layer chromatography, which was performed on aluminum sheets pre-coated with silica gel 60 (HF-254, Merck) to a thickness of 0.25 mm. The chromatograms were viewed under ultraviolet light (254–265 nm). For column chromatography Merck silica gel (70–230 mesh) was used. ^{1}H NMR spectra were determined in deuterated dimethyl sulfoxide using a Bruker DPX-200 at 200 MHz. ^{13}C NMR spectra were determined in this spectrometer at 50 MHz, employing the same solvent. Chemical shifts are given in parts per million (δ) from tretramethylsilane as internal standard, and coupling constant values (J) are given in Hertz (Hz). Signal multiplicities are represented by: s (singlet), d (doublet), t (triplet), q (quadruplet), m (multiplet) and br (broad signal). Infrared (IR) spectra were obtained with a FTLA 2000–100 spectrophotometer using potassium bromide plates.

Melting points of final products were determined with a Quimis 340 apparatus and are uncorrected. The purity of compounds

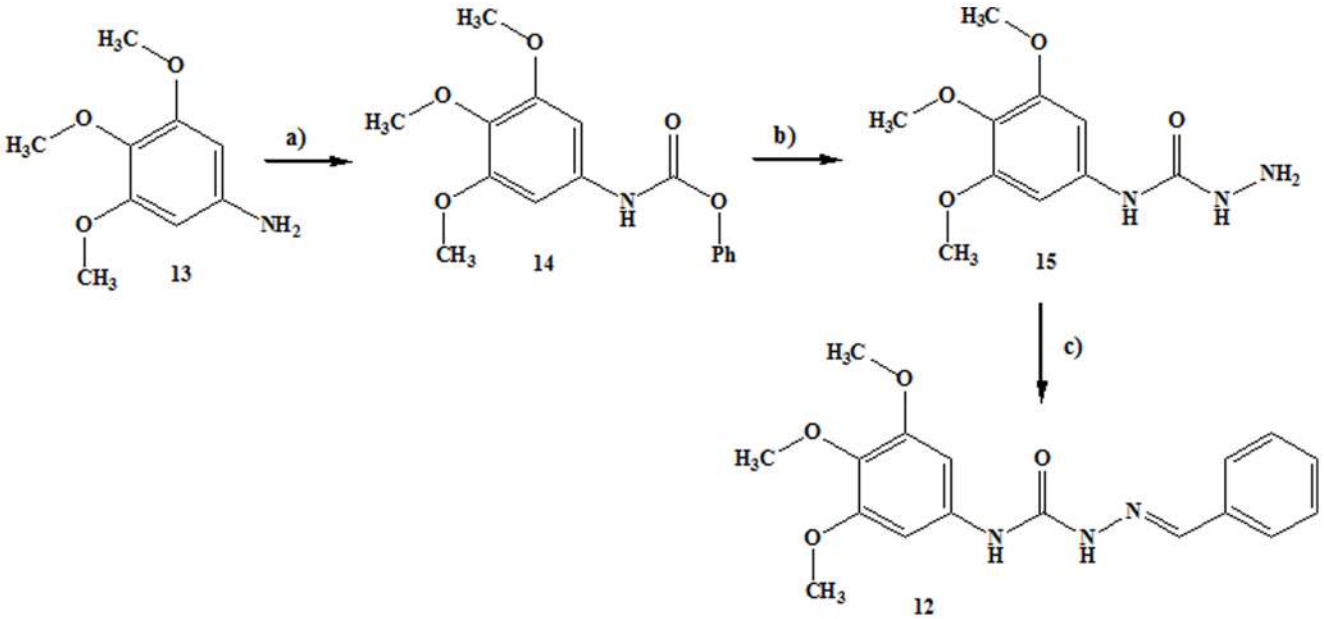

Figure 7. Conditions and reagents: a) Phenyl chloroformate, $CHCl_3$, reflux, 2 h, 47%; b) $N_2H_4.H_2O$, toluene, r.t., 72 h, 64%; c) PhCHO, EtOH, HCl (cat), r.t., 1 h, 83%.
doi:10.1371/journal.pone.0085380.g007

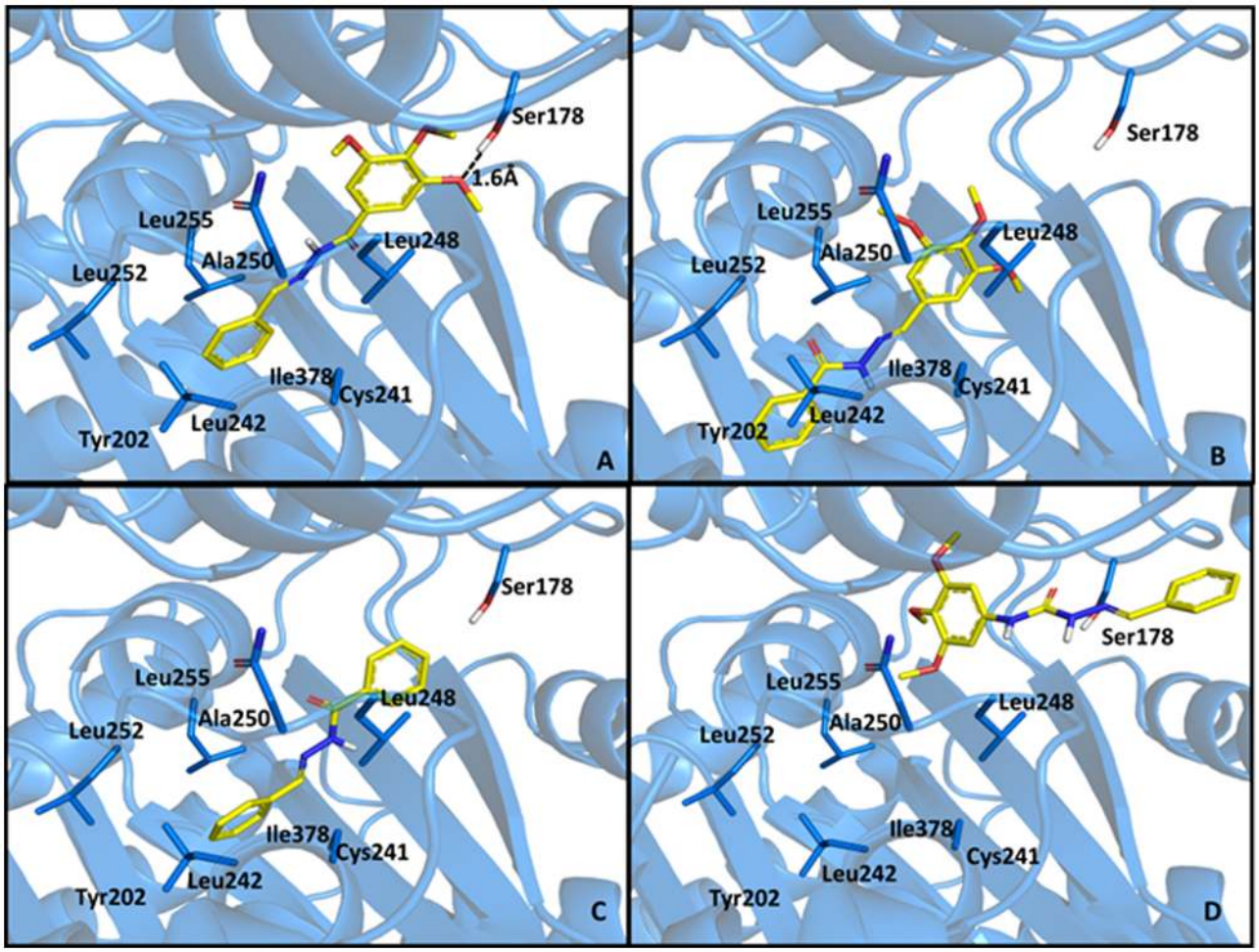

Figure 8. Best poses of compounds 5b (A), 10 (B), 9 (C) and 12 (D) at the colchicine binding pocket β-tubulin (PDB code: 1sa0).
doi:10.1371/journal.pone.0085380.g008

were determined by HPLC (>95%) using the Shimadzu – LC20AD apparatus, a Kromasil 100-5C18 (4,6 mm×250 mm) column and the SPD-M20A detector (Diode Array) at 254 nm for quantification of analyte in a 1 mL/min constant flux. The injector was programmed to inject a volume of 20 -μL. The mobile phases used were: CH_3CN:H_2O 1:1; 6:4 and 7:3.

Ultraviolet spectroscopy was performed using Femto spectrophotometer. The wavelength used in solubility assay was determined by the -λ max characteristic of each compound. Spectra were analyzed in Femtoscan software. Mass spectrometry was obtained by positive ionization at Bruker AmaZon SL and data analyzed in Compass 1.3.SR2 software.

General Procedure for the preparation of 3,4,5-trimethoxybenzohydrazide (8)

To a solution of methyl 3,4,5-trimethoxybenzoate (7) (2.00 g, 8.84 mmol) in absolute methanol (26 mL), 8.56 mL (176.8 mmol) of hydrazine hydrate 80% was added. The reaction mixture was

Table 4. Antiproliferative activity of compounds **CA-4**, **5b** and **9–12** against HL-60, SF295, HCT-8 and MDA-MB435 tumor cells.

IC_{50} (μM)				
Compound	**HL-60**	**SF295**	**HCT-8**	**MDA-MB435**
CA-4	0.0021	0.0062	0.0053	0.0079
5b	0.29	0.26	0.45	0.064
9	>25	>25	>25	>25
10	>25	>25	>25	>25
11	0.03	3.80	0.54	1.91
12	>25	>25	>25	>25

doi:10.1371/journal.pone.0085380.t004

Table 5. *In vivo* antiproliferative activity of **5b** and 5-fluorouracil (5-FU) in Hollow Fiber Assay (HFA).

Groups[1]	Dose (mg/kg/day)	Survival	Proliferation (OD595 nm)		Inhibition (%)	
			SF-295	HCT-116	SF-295	HCT-116
Control[2]	-	6/6	1.50±0.21	1.55±0.18	-	-
5-FU[3]	25	7/7	0.52±0.08*	0.59±0.10*	65.40	62.08
5b	25	7/7	0.57±0.05*	0.26±0.04*	61.89	82.89
	50	6/6	0.41±0.06*	0.29±0.05*	72.68	80.76

[1]The data are reported as the mean ± S.E.M., n = 6–7 animals/group, which were treated for 4 days intraperitoneally.
[2]The negative control group received 5% DMSO.
[3]5-Fluorouracil (5-FU) was used as the positive control.
*$P<0.05$ compared to the control by ANOVA, followed by Newman-Keuls test.
doi:10.1371/journal.pone.0085380.t005

kept under reflux for 5 hours, when TLC indicated the end of the reaction. Then, the media was poured into ice and the resulting precipitate was filtered out affording the 3,4,5-trimethoxybenzohydrazide in 88% yield, as a white solid, m.p. 166–168°C. The melting point, ^{1}H NMR, ^{13}C NMR and IR data are in agreement with previous reports [29]. I.R. (KBr) (cm^{-1}): 3392, 3335, 3294, 3196 $\nu_{sim.}$ and $\nu_{assim.}$ NH), 1656 (ν CO), 1614 (ν NH); ^{1}H NMR (200 MHz, DMSO-d_6) δ (ppm): 9.72 (1 H, s, NH), 7.16 (2 H, s, H2 & H6), 4.47 (2 H, br, NH_2), 3.81 (6 H, s, H3a & H5a), 3.69 (3 H, s, H4a); ^{13}C NMR (50 MHz, DMSO-d_6) δ (ppm): 165.4 (CO), 152.6 (C3 & C5), 139.8 (C4), 128.4 (C1), 104.5 (C2 & C6), 60.0 (C8), 55.9 (C7 & C9).

General Procedure for the preparation of 3,4,5-trimethoxybenzoyl-arylhydrazones (5a–r)

To a solution of 8 (0.2 g, 0.884 mmol) in absolute ethanol (7 mL) containing one drop of 37% hydrochloric acid, was added 0.884 mmol of corresponding aldehyde derivative. The mixture was stirred at room temperature until TLC indicated the end of reaction (0.5–4 h). Then the mixture was poured into ice and the precipitate was filtered out and dried. Yields and characterization pattern are described below:

***(E)-N′*-(4-hydroxy-3-methoxybenzylidene)-3,4,5-trimetoxybenzohydrazide (5a; LASSBio-1593).** Yield: 72%, white solid, m.p. 117–120°C; I.R. (KBr) cm^{-1}: 3220 (ν NH), 1635 (ν CO), 1579 (ν CN); ^{1}H NMR (200 MHz, DMSO-d_6) δ (ppm): 11.56 (1 H, s, NH), 9.35 (1 H, s, OH), 8.30 (1 H, s, N = CH), 7.28 (1 H, s, H2′), 7.22 (2H, s, H2 & H6), 7.08 – 6.95 (2 H, m, H5′ & H6′), 3.85 (6 H, s, H3a & H5a), 3.80 (3 H, s, H4a′), 3.72 (3 H, s, H4a); ^{13}C NMR (50 MHz, DMSO-d_6) δ (ppm): 162.4 (CO), 152.7 (C3 & C5), 149.9 (C4′), 148.0 (CN), 146.9 (C3′), 140.4 (C4), 128.7 (C1′), 127.2 (C1), 120.3 (C6′), 112.4 (C2′), 111.9 (C5′), 105.2 (C2 & C6), 60.2 (C4a), 56.1 (C3a & C5a), 55.6 (C4′a). 99.6% purity in HPLC (R.T. = 3.03 min; CH_3CN:H_2O (7:3)). MS: m/z = 361.1 $(M+H)^+$.

***(E)-N′* benzylidene-3,4,5-trimetoxybenzohydrazide (5b; LASSBio-1586).** Yield: 76%, white solid, m.p. 131–134°C The melting point, ^{1}H NMR, ^{13}C NMR and IR data are in agreement with previous reports [29]. I.R. (KBr) (cm^{-1}): 3183 (ν NH), 1648 (ν CO), 1584 (ν CN); ^{1}H NMR (200 MHz, DMSO-d_6) δ (ppm): 11.73 (1 H, s, NH), 8.48 (1 H, s, N = CH), 7.73 (2 H, d, J = 2 Hz, H2′ & H6′), 7.47- 7.45 (3 H, m, H3′,H4′ & H5′), 7.25 (2 H, s, H2 & H6), 3.87 (6 H, s, H3a & H5a), 3.73 (3 H, s, H4a); ^{13}C NMR (50 MHz, DMSO-d_6) δ (ppm): 162.6 (CO), 152.7 (C3 & C5), 147.8 (CN), 140.5 (C4), 134.3 (C1′), 130.0 (C4′), 128.8 (C2′ & C6′), 128.5 (C1), 127.0 (C3′ & C5′), 105.3 (C2 & C6), 60.1 (C4a), 56.1 (C3a & C5a). 99.4% purity in HPLC (R.T. = 3.89; CH_3CN:H_2O (7:3)). MS: m/z = 315.1 $(M+H)^+$.

***(E)-N′*-(3-hydroxybenzylidene)-3,4,5-trimetoxybenzohydrazide (5c; LASSBio-1587).** Yield: 83%, cream solid, m.p. 227–229°C; I.R. (KBr) (cm^{-1}): 3462 (ν OH), 3280 (ν NH), 1665 (ν CO), 1587 (ν CN); ^{1}H NMR (200 MHz, DMSO-d_6) δ (ppm): 11.68 (1 H, s, NH), 9.68 (1 H, s, OH), 8.37 (1 H, s, N = CH), 7.23 (4 H, m, H2, H6,), 7.11 (2 H, d, J = 10 Hz, H4′), 6.84 (2 H, d, J = 6 Hz, H6′), 3.86 (6 H, s, H3a & H5a), 3.73 (3 H, s, H4a); ^{13}C NMR (50 MHz, DMSO-d_6) δ (ppm): 162.6 (CO), 157.7 (C3′), 152.7 (C3 & C5), 147.9 (CN), 140.5 (C4), 135.6 (C1′), 129.9 (C5′), 128.5 (C1), 118.8 (C6′), 117.5 (C4′), 112.7 (C2′), 105.3 (C2 & C6), 60.2 (C4a), 56.1 (C5a & C3a). 97.5% purity in HPLC (R.T. = 3.12; CH_3CN:H_2O (7:3)). MS: m/z = 331.1 $(M+H)^+$.

***(E)-N′*-(4-hydroxybenzylidene)-3,4,5-trimetoxybenzohydrazide (5d; LASSBio-1588).** Yield: 65%, pale yellow solid, m.p. 189°C; I.R. (KBr) cm^{-1}: 3382 (ν OH), 3279 (ν NH), 1638 (ν CO), 1584 (ν CN); ^{1}H NMR (200 MHz, DMSO-d_6) δ (ppm): 11.51 (1 H, s, NH), 9.94 (1 H, s, OH), 8.36 (1 H, s, N = CH), 7.57 (2 H, d, J = 8 Hz, H3′ & H5′), 7.22 (1 H, s, H2 & H6), 6.84 (2H, d, J = 8 Hz, H2′ & H6′), 3.86 (6 H, s, H3a & H5a), 3.72 (3 H, s, H4a); ^{13}C NMR (50 MHz, DMSO-d_6) δ (ppm): 162.3 (CO), 159.4 (C4′), 152.7 (C3 & C5), 148.2 (CN), 140.3 (C4), 128.8 (C3′ & C5′), 128.7 (C1), 125.3 (C1′), 115.8 (C2′ & C6′), 105.2 (C2 & C6), 60.1 (C4a), 56.1 (C3a & C5a). 95.7% purity in HPLC (R.T. = 3.26 min; CH_3CN:H_2O (6:4)). MS: m/z = 331.1 $(M+H)^+$.

***(E)-N′*-(3,4-dihydroxybenzylidene)-3,4,5-trimetoxybenzohydrazide (5e; LASSBio-1589).** Yield: 85%, white solid, m.p. 160°C; I.R. (KBr) cm^{-1}: 3435 (ν OH), 3215 (ν NH), 1649 (ν CO), 1582 (ν CN); ^{1}H NMR (200 MHz, DMSO-d_6) δ (ppm): 11.48 (1 H, s, NH), 9.35 (2 H, sl, OH), 8.27 (s, 1 H, N = CH), 7.22 (3 H, m, H2, H6 & H2′), 6.95 (1H, d, J = 6 Hz, H5′), 6.89 (1H, d, J = 8 Hz, H6′), 3.86 (6 H, s, H3a & H5a), 3.72 (3 H, s, H4a); ^{13}C NMR (50 MHz, DMSO-d_6) δ (ppm): 162.2 (CO), 152.7 (C3 & C5), 148.3 (CN), 148.0 (C4′), 145.7 (C3′), 140.3 (C4), 128.7 (C1′), 125.7 (C1), 120.5 (C6′), 115.6 (C5′), 122.7 (C2′), 105.1 (C2 &C6), 60.1 (C4a), 56.1 (C3a & C5a). 99.0% purity in HPLC (R.T. = 2.88 min; CH_3CN:H_2O (7:3)). MS: m/z = 347.1 $(M+H)^+$.

***(E)-N′*-(3-hydroxy-4-methoxybenzylidene)-3,4,5-trimetoxybenzohydrazide (5f; LASSBio-1592).** Yield: 62%, yellow solid, m.p. 210°C. The melting point, ^{1}H NMR, ^{13}C NMR and IR data are in agreement with previous reports [31]. I.R. (KBr) cm^{-1}: 3223 (ν NH), 1638 (ν CO), 1582 (ν CN); ^{1}H NMR (200 MHz, DMSO-d_6) δ (ppm): 11.55 (1 H, s, NH), 9.56 (1 H, s, OH), 8.36 (1 H, s, N = CH), 7.32 (1 H, s, H2′), 7.23 (2 H, s, H2 & H6), 7.09 (1 H, d, J = 8 Hz, H5′), 6.85 (1H, d, J = 8 Hz, H6′), 3.86 (6 H, s, H3a & H5a), 3.83 (3 H, s, H3a′), 3.73 (3 H, s, H4a); ^{13}C NMR (50 MHz, DMSO-d_6) δ (ppm): 162.3 (CO), 152.6 (C3 &C5), 149.0 (C4′),

148.4 (CN), 148.0 (C3′), 140.3 (C4), 128.7 (C1′), 125.7 (C1), 122.1 (C6′), 115.4 (C5′), 109.0 (C2′), 105.1 (C2 & C6), 60.1 (C4a), 56.1 (C3a & C5a), 55.5 (C3′a). 97.3% purity in HPLC (R.T. = 3.32 min; CH_3CN:H_2O (6:4)). MS: m/z = 361.1 $(M+H)^+$.

***(E)*-*N*′-(3,4-dimethoxybenzylidene)-3,4,5-trimetoxybenzohydrazide (5g; LASSBio-1590).** Yield: 86%, pale yellow solid, m.p. 190–191°C; I.R. (KBr) cm^{-1}: 3221 (ν NH), 1647 (ν CO), 1582 (ν CN); ^1H NMR (200 MHz, DMSO-d_6) δ (ppm): 11.62 (1 H, s, NH), 8.40 (1 H, s, N = CH), 7.35 (1 H, s, H2′), 7.23 – 7.19 (3 H, m, H2, H6 & H5′), 7.03 (1H, d, J = 8 Hz, H6′), 3.86 (6 H, s, H3a & H5a), 3.81 (6 H, s, H3a′ & H4a′), 3.72 (3 H, s, H4a); ^{13}C NMR (50 MHz, DMSO-d_6) δ (ppm): 162.4 (CO), 152.7 (C3 & C5), 150.8 (C4′), 149.1 (C3′), 148.1 (CN), 140.5 (C4), 128.6 (C1′), 127.0 (C1), 121.8 (C6′), 111.5 (C2′), 108.3 (C4′), 105.2 (C2 & C6), 60.1 (C4a), 56.1(C3′a & C5′a), 55.5 (C4′a), 55.4 (C3′a). 97.6% purity in HPLC (R.T. = 3.78 min; CH_3CN:H_2O (6:4)). MS: m/z = 375.2 $(M+H)^+$.

***(E)*-*N*′-(benzo[*d*][1,3]dioxol-5-ylmethylene)-3,4,5-trimetoxybenzohydrazide (5h; LASSBio-1591).** Yield: 70%, white solid, m.p. 222–223°C. The melting point, ^1H NMR, ^{13}C NMR and IR data are in agreement with previous reports [30]. I.R. (KBr) cm^{-1}: 3223 (ν NH), 1638 (ν CO), 1582 (ν CN); ^1H NMR (200 MHz, DMSO-d_6) δ (ppm): 11.63 (1 H, s, NH), 8.38 (1 H, s, N = CH), δ 7.31 (1 H, s, H4′), 7.23 – 7.16 (3 H, m, H2, H6 & H6′), 6.99 (1H, d, J = 8 Hz, H7′), 6.09 (2 H, s, O-CH_2-O), 3.86 (6 H, s, H3a & H5a), 3.72 (3 H, s, H4a); ^{13}C NMR (50 MHz, DMSO-d_6) δ (ppm): 162.4 (CO), 152.7 (C3 & C5), 149.1 (C3′a), 148.0 (C7′a), 147.6 (CN), 140.4 (C4), 128.7 (C1′), 128.6 (C1), 123.2 (C6′), 108.2 (C4′), 104.6 (C2 & C6), 101.5 (C2′), 60.1 (C4a), 56.1 (C3a & C5a). 97.9% purity in HPLC (R.T. = 5.94 min; CH_3CN:H_2O (1:1)). MS: m/z = 359.1 $(M+H)^+$.

***(E)*-3,4,5-trimethoxy-*N*′-(3,4,5-trimethoxybenzylidene)benzohydrazide (5i; LASSBio-1594).** Yield: 92%, pale yellow solid, m.p. 232°C The melting point, ^1H NMR, ^{13}C NMR and IR data are in agreement with previous reports [30]. I.R. (KBr) cm^{-1}: 3210 (ν NH), 1641 (ν CO), 1579 (ν CN); ^1H NMR (200 MHz, DMSO-d_6) δ (ppm): 11.71 (1 H, s, NH), 8.42 (1 H, s, N = CH), 7.23 (2 H, s, H2 & H6), 7.03 (2 H, s, H2′ & H6′), 3.86/3.84 (12 H, 2s, H3a, H5a, H3a′ & H5a′), 3.73/3.71 (6 H, 2s, H4a & H4a′); ^{13}C NMR (50 MHz, DMSO-d_6) δ (ppm): 162.6 (CO), 153.2 (C3 & C5), 152.6 (C3′ & C5′), 147.9 (CN), 140.4 (C4), 139.1 (C4′), 129.8 (C1), 128.6 (C1′), 105.2 (C2 & C6), 104.3 (C2′ & C6′), 60.1 (C4a & C4′a), 56.1 (C3a & C5a), 55.9 (C3′a & C5′a). 96.0% purity in HPLC (R.T. = 3.41 min; CH_3CN:H_2O (7:3)). MS: m/z = 405.2 $(M+H)^+$.

***(E)*-3,4,5-trimethoxy-*N*′-((4-oxo-4H-chromen-3-yl)methylene)-benzohydrazide (5j; LASSBio-1595).** Yield: 95%, pale yellow solid, m.p. 205–206°C. I.R. (KBr) cm^{-1}: 3222 (νNH), 1640 (ν CO), 1584 (ν CN); ^1H NMR (200 MHz, DMSO-d_6) δ (ppm): 11.80 (1 H, s, NH), 8.84 (1 H, s, N = CH), 8.65 (1 H, s, H2′), 8.13 (1 H, d, J = 8 Hz, H8′), 7.86 (1 H, t, J = 8 Hz, H6′), 7.72 (1 H, d, J = 8 Hz, H5′), 7.55 (1 H, t, J = 8 Hz, H7′), 7.26 (2 H, s, H2 & H6), 3.87 (6 H, s, H3a & H5a), 3.57 (3 H, s, H4a); ^{13}C NMR (50 MHz, DMSO-d_6) δ (ppm): 175.1 (C1′), 162.2 (CO), 155.7 (C3′), 154.5 (C4′a), 152.7 (C3 & C5), 140.5 (CN), 140.1 (C4), 134.6 (C6′), 128.1 (C1), 128.0 (C8′), 125.2 (C8′a), 123.3 (C7′), 118.7 (C5′), 118.3 (C2′), 105.2 (C2 & C6), 60.1 (C4a), 56.1 (C3a, C5a). 98.0% purity in HPLC (R.T. = 3.49 min; CH_3CN:H_2O (7:3)). MS: m/z = 383.1 $(M+H)^+$.

***(E)*-*N*′-(3,5-di-tert-butyl-4hydroxybenzylidene)-3,4,5-trimetoxybenzohydrazide (5k; LASSBio-1596).** Yield: 67% after column chromatographic (dichloromethane: methanol), pale yellow solid, m.p. 222–224°C. I.R. (KBr) cm^{-1}: 3207 (ν NH), 1646 (ν CO), 1583 (νCN); ^1H NMR (200 MHz, DMSO-d_6) δ (ppm): 11.49 (1 H, s, NH), 8.42 (1 H, s, N = CH), 7.48 (2 H, s, H2′ & H6′), 7.43 (1 H, s, OH), 7.23 (2 H, s, H2 & H6), 3.86 (6 H, s, H3a & H5a), 3.72 (3 H, s, H4a), 1.41 (18H, s, H5b′ & H3b′); ^{13}C NMR (50 MHz, DMSO-d_6) δ (ppm): 162.2 (CO),156.1 (C4′), 152.6 (C3 & C5), 149.4 (CN), 140.3 (C4), 139.4 (C3′ & C5′), 128.7 (C1), 125.5 (C1′), 123.87 (C2′ & C6′), 105.1 (C2 &C6), 60.1 (C4a), 56.0 (C3a & C5a), 34.4 (3a′), 30.1 (3b′). 98.9% purity in HPLC (R.T. = 7.56 min; CH_3CN:H_2O (7:3)). MS: m/z = 443.3 $(M+H)^+$.

***(E)*-3,4,5-trimetoxy-*N*′-(naphtalen-1-ylmethylene) benzohydrazide (5l; LASSBio-1738).** Yield: 88%, white solid, m.p. >250°C The melting point, ^1H NMR, ^{13}C NMR and IR data are in agreement with previous reports [32]. I.R. (KBr) cm^{-1}: 3226 (ν NH), 1646 (ν CO), 1591 (ν CN); ^1H NMR (200 MHz, DMSO-d_6) δ (ppm): 11.84 (1 H, s, NH), 9.12 (1 H, s, N = CH), 8.89 (1 H, d, J = 8 Hz, H2′), 8.04 – 7.93 (3 H, m, H4′, H5′ & H8′), 7.68 – 7.57 (3 H, m, H3′, H6′ & H7′), 7.31 (2 H, s, H2 & H6), 3.89 (6 H, s, H3a & H5a), 3.75 (3H, s, H4a); ^{13}C NMR (50 MHz, DMSO-d_6) δ (ppm): 162.6 (CO), 152.7 (C3 & C5), 147.4 (CN), 140.5 (C4), 133.5 (C4′a), 130.5 (C4′), 130.1 (C8′a), 129.6 (C1), 128.8 (C1′), 128.5 (C5′), 127.7 (C3′), 127.2 (C6′), 126.2 (C7′), 125.5 (C2′), 124.0 (C8′), 105.3 (C2 & C6), 60.1 (C4a), 56.1 (C3a, C5a). 97.0% purity in HPLC (R.T. = 4.95 min; CH_3CN:H_2O (7:3)). MS: m/z = 365.2 $(M+H)^+$.

***(E)*-3,4,5-trimetoxy-*N*′-(naphtalen-2-ylmethylene) benzohydrazide (5m; LASSBio-1739).** Yield: 89%, white solid, m.p. >250°C. The melting point, ^1H NMR, ^{13}C NMR and IR data are in agreement with previous reports [32]. I.R. (KBr) cm^{-1}: 3176 (ν NH), 1645 (ν CO), 1578 (ν CN); ^1H NMR (200 MHz, DMSO-d_6) δ (ppm): 11.84 (1 H, s, NH), 8.63 (1 H, s, N = CH), 8.15 (1 H, s, H1′), 8.04 (4 H, m, H3′, H4′, H5′ & H8′), 7.59 – 7.55 (2 H, m, H6′ & H7′), 3.88 (6 H, s, H3a & H5a), 3.74 (3H, s, H4a); ^{13}C NMR (50 MHz, DMSO-d_6) δ (ppm): 162.6 (CO), 152.6 (C3 & C5), 147.6 (CN), 133.7 (C4′a), 132.8 (C1′), 132.0 (C2′), 128.5 (C8′a), 128.5 (C8′ & C1), 128.3 (C6′), 127.7 (C4′), 127.1 (C5′), 126.7 (C7′), 122.6 (C3′), 105.2 (C2 & C6), 60.1 (C4a), 56.1 (C3a, C5a). 98.1% purity in HPLC (R.T. = 5.03 min; CH_3CN:H_2O (7:3)). MS: m/z = 365.2 $(M+H)^+$.

***(E)*-*N*′-(biphenyl-4-ylmethylene)-3,4,5- trimethoxyibenzohydrazide (5n; LASSBio-1740).** Yield: 87%, white solid, m.p. 187–188°C. I.R. (KBr) cm^{-1}: 3204 (ν NH), 1644 (ν CO), 1585 (ν CN); ^1H NMR (200 MHz, DMSO-d_6) δ (ppm): 11.77 (1 H, s, NH), 8.52 (1 H, s, N = CH), 7.86 – 7.71 (6 H, m, H3′, H5′, H2′, H6′, H6′a & H2′a), 7.52 – 7.39 (3 H, m, H3′a, H4′a & H5′a), 3.87 (H3a & H5a), 3.74 (H4a); ^{13}C NMR (50 MHz, DMSO-d_6) δ (ppm): 162.6 (CO), 152.7 (C3 & C5), 147.3 (CN), 141.6 (C1′), 140.5 (C4), 139.3 (C1′a), 133.4 (C4′), 129.0 (C3′ & C5′), 128.5 (C3′a & C5′a), 127.8 (C1), 127.6 (C2′ & C6′), 127.0 (C2′a & C6′a), 126.6 (C4′a), 105.3 (C2 & C6), 60.1 (C4a), 56.1 (C3a, C5a). 98.8 purity in HPLC (R.T. = 5.57 min; CH_3CN:H_2O (7:3)). MS: m/z = 391.2 $(M+H)^+$.

***(E)*-3,4,5-trimethoxy-*N*′-(4-methylbenzylidene) benzohydrazide (5o; LASSBio-1741).** Yield: 83%, white solid, m.p. 189–190°C The melting point, ^1H NMR, ^{13}C NMR and IR data are in agreement with previous reports [32]. I.R. (KBr) cm^{-1}: 3208 (ν NH), 1644 (ν CO), 1586 (ν CN); ^1H NMR (200 MHz, DMSO-d_6) δ (ppm): 11.66 (1 H, s, NH), 8.43 (1 H, s, N = CH), 7.63 (2 H, d, J = 8 Hz, H2′ & H6′), 7.29 – 7.24 (4 H, m, H3′, H5′, H2 & H6), 3.86 (6 H, s, H3a & H5a), 3.73 (3 H, s, H4a), 2.34 (3H, s, H4′a); ^{13}C NMR (50 MHz, DMSO-d_6) δ (ppm): 162.5 (CO), 152.7 (C3 & C5), 147.9 (CN), 140.5 (C4), 139.9 (C4′), 131.6 (C1′), 129.5 (C3′ & C5′), 128.6 (C1), 127.1 (C2′ & C6′), 105.2 (C2 & C6), 60.1 (C4a), 56.1 (C3a, C5a), 21.1 (C4′a). 96.7% purity in HPLC (R.T. = 4.12 min; CH_3CN:H_2O (7:3)). MS: m/z = 315.1 $(M+H)^+$.

***(E)*-*N*′-(4-fluorobenzylidene) - 3,4,5-trimetoxybenzohyidrazide (5p; LASSBio-1742).** Yield: 82%, white solid,

m.p.181–182°C The melting point, ^{1}H NMR, ^{13}C NMR and IR data are in agreement with previous reports [30]. I.R. (KBr) cm^{-1}: 3185 (ν NH), 1649 (ν CO), 1588 (ν CN); ^{1}H NMR (200 MHz, DMSO-d_6) δ (ppm): 11.78 (1 H, s, NH), 8.47 (1 H, s, N = CH), 7.83 – 7.76 (2 H, m, H2′ & H6′), 7.35 – 7.24 (4 H, m, H3′, H5′, H2 & H6), 3.86 (6 H, s, H3a & H5a), 3.73 (3 H, s, H4a); ^{13}C NMR (50 MHz, DMSO-d_6) δ (ppm): 165.5 – 160.6 (C4′, J_{CF} = 246 Hz), 162.5 (CO), 152.7 (C3 & C5), 146.6 (CN), 140.5 (C4), 130.9 (C1′), 129.3 – 129.1 (C2′ & C6′, J_{CF} = 8,5 Hz), 128.4 (C1), 116.1 – 115.7 (C3′ & C5′, J_{CF} = 21,5 Hz), 105.2 (C2 & C6), 60.1 (C4a), 56.1 (C3a, C5a). 98.0% purity in HPLC (R.T. = 3.79 min; CH_3CN:H_2O (7:3)). MS: m/z = 333.1 $(M+H)^+$.

***(E)-N′*-(4-chlorobenzylidene)-3,4,5-trimetoxybenzohyidrazide (5q; LASSBio-1743).** Yield: 83%, white solid, m.p.187–188°C. The melting point, ^{1}H NMR, ^{13}C NMR and IR data are in agreement with previous reports [32]. I.R. (KBr) cm^{-1}: 3235 (ν NH), 1647 (ν CO), 1582 (ν CN), 1079 (ν Ar-Cl); ^{1}H NMR (200 MHz, DMSO-d_6) δ (ppm): 11.78 (1 H, s, NH), 8.46 (1 H, s, N = CH), 7.76 (2 H, d, J = 8 Hz, H2′ & H6′), 7.52 (2 H, d, J = 8 Hz, H3′& H5′), 7.24 (2 H, s, H2 & H6), 3.86 (6 H, s, H3a & H5a), 3.73 (3 H, s, H4a); ^{13}C NMR (50 MHz, DMSO-d_6) δ (ppm): 162.6 (CO), 152.7 (C3 & C5), 146.4 (CN), 140.5 (C4), 134.5 (C4′), 133.2 (C1′), 128.9 (C3′ & C5′), 128.6 (C2′& C6′), 128.3 (C1), 105.3 (C2 & C6), 60.1 (C4a), 56.1 (C3a, C5a). 97.5% purity in HPLC (R.T. = 4.36 min; CH_3CN:H_2O (7:3)). MS: m/z = 349.1 $(M+H)^+$ and 351.1 $([M+2]+H)^+$.

***(E)-N′*-(4-bromobenzylidene) - 3,4,5-trimetoxybenzohyidrazide (5r; LASSBio-1744).** Yield: 78%, white solid, m.p.214–215°C. The melting point, ^{1}H NMR, ^{13}C NMR and IR data are in agreement with previous reports [30]. I.R. (KBr) cm^{-1}: 3263 (ν NH), 1664 (ν CO), 1587 (ν CN), 1067 (ν Ar-Br); ^{1}H NMR (200 MHz, DMSO-d_6) δ (ppm): 11.78 (1 H, s, NH), 8.44 (1 H, s, N = CH), 7.67 (4 H, s, H2′, H3′, H5′ & H6′), 7.24 (2 H, s, H2 & H6), 3.86 (6 H, s, H3a & H5a), 3.73 (3 H, s, H4a); ^{13}C NMR (50 MHz, DMSO-d_6) δ (ppm): 162.5 (CO), 152.6 (C3 & C5), 146.4 (CN), 140.5 (C4), 133.6 (C1′), 131.8 (C3′ & C5′), 128.8 (C2′ & C6′), 128.3 (C1), 123.2 (C4′), 105.3 (C2 & C6), 60.1 (C4a), 56.1 (C3a, C5a).98.5% purity in HPLC (R.T. = 4.74; CH_3CN:H_2O (7:3)). MS: m/z = 393.1 $(M+H)^+$ and 395.1 $([M+2]+H)^+$.

Benzohydrazide

A solution of benzoic acid (2.0 g, 16.4 mmol) in 50 mL of methanol, containing 5 drops of sulfuric acid, were refluxed with a Dean-Stark apparatus for 5 hours to obtain the corresponding methyl ester. Then, 328 mmol of hydrazine hydrate 80% were added to the reaction mixture and kept under reflux for 2 hours to obtain benzohydrazide in a one-pot methodology in 94% yield as a white solid, m.p. 112–114°C. The melting point data is in agreement with previous reports [33].

***(E)-N′*-benzylidenebenzohydrazide (9; LASSBio-372).** Yield: 53%, cream solid, m.p. 211–212°C. The melting point, ^{1}H NMR, ^{13}C NMR and IR data are in agreement with previous reports [34]. I.R. (KBr) cm^{-1}: 3181 (ν NH), 1641 (ννCO), 1600 (ν CN); ^{1}H NMR (200 MHz, DMSO-d_6) δ (ppm): 11.86 (1 H, s, NH), 8.48 (1 H, s, N = CH), 7.93 (2 H, d, J = 6 Hz, H2 & H6), 7.73 (2 H, d, J = 4 Hz, H2′ & H6′), 7.60 – 7.45 (6 H, m, H3, H4, H5, H5′, H4′ & H3′); ^{13}C NMR (50 MHz, DMSO-d_6) δ (ppm): 163.1 (CO), 147.7 (CN), 134.3 (C1), 133.4 (C1′), 131.6 (C4), 130.0 (C4′), 128.8 (C2 & C6), 128.4 (C2′ & C6′), 127.5 (C3 & C5), 127.0 (C3′ & C5′); 97.8% purity in HPLC (R.T. = 3.78; CH_3CN:H_2O (7:3)). MS: m/z = 225.1 $(M+H)^+$.

***(E)-N′*-(3,4,5-trimethoxybenzylidene)-benzohydrazide (10; LASSBio-1734).** Yield: 56%, cream solid, m.p. 211–212°C; I.R. (KBr) cm^{-1}: 3239 (ν NH), 1649 (ν CO), 1575 (ν CN); RMN ^{1}H (200 MHz, DMSO-d_6) δ (ppm): 11.86 (1 H, s, NH), 8.39 (1 H, s, N = CH), 7.91 (2 H, d, J = 8 Hz, H2 & H6), 7.62 -7.51 (3 H, m, H3, H4 & H5), 7.03 (2 H, s, H2′ & H6′), 3.84 (6 H, s, C3′a & C5′a), 3.35 (C4′a); ^{13}C NMR (50 MHz, DMSO-d_6) δ (ppm): 163.1 (CO), 153.1 (C3′ & C5′), 147.8 (CN), 139.2 (C4′), 133.5 (C1), 131.6 (C1′), 129.8 (C4), 128.4 (C2 & C6), 127.6 (C3 & C5), 104.3 (C2′ & C6′), 60.1 (C4′a), 55.9 (C3′a & C5′a); 98.3% purity in HPLC (R.T. = 3.47; CH_3CN:H_2O (7:3)). MS: m/z = 315.1 $(M+H)^+$.

***(E)- N′*-benzylidene-3,4,5-trimethoxy-*N*-methylbenzohydrazide (11; LASSBio-1735).** To a solution of LASSBio-1586 (0.4 g, 1.27 mmol) in 7 mL of acetone was added 3.82 mmol of sodium carbonate. The resultant suspension was stirred at room temperature for 50 minutes. Then, methyl iodide (0.48 mL, 7.63 mmol) was added to the suspension and the reaction mixture was heated for 24 hours at 40°C. After total conversion of reactant to product, the acetone were removed under reduced pressure and then the material were suspended in 2 mL of ethanol, filtered and washed with petroleum ether. Recrystallization of the *N*-methylated product was performed in ethanol/water mixture. LASSBio-1735 was obtained in 94% of yield as a white crystalline solid with cotton aspect. m.p.71–73°C; I.R. (KBr) cm^{-1}: 1648 (ν CO), 1592 (ν CN); ^{1}H NMR (200 MHz, DMSO-d_6) δ (ppm): 8.04 (1 H, s, N = CH), 7.58 (2 H, d, J = 8 Hz, H2′ & H6′), 7.41 – 7.38 (3 H, m, H3′, H4′ & H5′), 7.00 (2 H, s, H2 & H6), 3.77 (6 H, s, H3a & H5a), 3.75 (3 H, s, H4a), 3.50 (3 H, s, NCH_3); ^{13}C NMR (50 MHz, DMSO-d_6) δ (ppm): 169.1 (CO), 151.8 (C3 & C5), 140.4 (CN), 139.2 (C4), 134.9 (C1′), 130.3 (C4′), 129.5 (C1), 128.7 (C2′ & C6′), 126.8 (C3′ & C5′), 107.6 (C2 & C6), 60.1 (C4a), 55.9 (C3a & C5a); 97.8% purity in HPLC (R.T. = 5.53; CH_3CN:H_2O (7:3)). MS: m/z = 329.1 $(M+H)^+$.

Synthesis of phenyl 3,4,5-trimetoxyphenylcarbamate (14)

3,4,5-trimethoxy aniline, **13**, (2.0 g, 10.92 mmol) dissolved in 20 mL of chloroform were add drop wised to a solution of phenylchloroformate (1.4 mL, 10.92 mmol) in 20 mL of chloroform. The resultant suspension was refluxed until total conversion of aniline to the corresponding carbamate. When at room temperature, 15 mL of *n*-hexane were added and the suspension were filtered under vacuum and washed with *n*-hexane. The compound **14** was obtained in 48% yield as cream needles, m.p. 170–171°C. The melting point, ^{1}H NMR, ^{13}C NMR and IR data are in agreement with previous reports [35]. I.R. (KBr) cm^{-1}: 3334 (ν NH), 1717 (ν CO); ^{1}H NMR (200 MHz, DMSO-d_6) δ (ppm): 10.12 (1 H, s, Ar-NH), 7.46 – 7.39 (2 H, m, H3′ & H5′), 7.29 – 7.18 (3 H, m, H2′, H4′ & H6′), 6.88 (2 H, s, H2 & H6), 3.73 (6 H, s, H3a & H5a), 3.62 (3 H, s, H4a); ^{13}C NMR (50 MHz, DMSO-d_6) δ (ppm): 152.9 (C3 & C5), 151.8 (C1′), 150.5 (CO), 134.7 (C4), 133.4 (C1), 129.4 (C3′ & C5′), 125.5 (C4′), 122.0 (C2′ & C6′), 96.5 (C2 & C6), 60.1 (C4a), 55.8 (C3a & C5a).

Synthesis of *N*-(3,4,5-trimetoxyphenyl) hydrazine carboxamide (15)

To a suspension of 14 (0.6 g, 1.98 mmol) in 15 mL of dry toluene, was added 29.7 mmol of hydrazide hydrate 64% and the mixture was stirred at room temperature until conversion of carbamate to correspondent semicarbazide. The product was filtered under vacuum, washed with *n*-hexane and obtained as a brown solid in 90% yield, m.p. >250°C; I.R.(KBr) cm^{-1}: 3582, 3459, 3346, 3145 (ν NH), 1718 (ν CO-ester), 1684 (ν CO amide); ^{1}H NMR (200 MHz, DMSO-d_6) δ (ppm): 8.83 (1 H, s, NH), 7.75 (1 H, Ar-NH), 6.89 (2 H, s, H2 & H6), 3.71 (11 H, br, NH_2, H3a, H4a, H5a); ^{13}C NMR (50 MHz, DMSO-d_6) δ (ppm): 156.9 (CO), 152.8 (C3 & C5), 135.9 (C4), 132.5 (C1), 96.2 (C2 & C6), 60.2 (C4a), 55.8 (C3a & C5a).

***(E)*-2-benzylidene-*N*-(3,4,5-trimetoxyphenyl) hydrazinecarboxamide (12; LASSBio-1714).** To a solution of 15 (0.2 g, 0.83 mmol) in etanol (7 mL), containing one drop of 37% chloridric acid, was added 0.83 mmol of benzaldehyde. The mixture was stirred at room temperature until TLC indicates the end of reaction. The mixture was poured into ice and the precipitate was filtered out and dried. LASSBio-1714 was obtained as a white solid in 83% yield, m.p. 217°C; I.R. (KBr) cm^{-1}: 3371, 3193 (ν NH), 1685 (ν CO); ^{1}H NMR (200 MHz, DMSO-d_6): δ 10.73 (1 H, s, NH), 8.79 (1 H, s, Ar-NH), 7.97 (1 H, s, N = CH), 7.85 (2 H, d, J = 6 Hz, H2′ & H6′), 7.44 – 7.41 (3 H, m, H3′, H4′ & H5′), 7.11 (2 H, s, H2 & H6), 3.76 (6 H, s, H3a & H5a), 3.62 (3H, s, H4a); ^{13}C NMR (50 MHz, DMSO-d_6): δ 152.9 (CO), 152.6 (C3 & C5), 140.9 (CN), 135.2 (C4), 134.2 (C4′), 132.9 (C1′), 129.4 (C1), 128.6 (C2′ & C6′), 127.0 (C3′ & C5′) 97.7 (C2 & C6), 60.1 (C4a), 55.8 (C3a & C5a); 99.0% purity in HPLC (R.T. = 4.23 min; CH_3CN:H_2O (7:3)). MS: m/z = 330.1 $(M+H)^+$.

X-ray Crystallography

A colorless prismatic single crystal of the compound LASSBio-1586, suitable for x-ray study, was obtained by slow evaporation of a solution of methanol-dimethylformamide (2:1) at room temperature 295(2) K. Data collection was performed using the Kappa Apex II Duo diffractometer operating with Cu-Kα radiation at 100 K. 8336 data points were collected of what 2687 are symmetry independent (R_{int} = 0.044). The molecule crystallizes in the $Pca2_1$ space group, having Z = 4. Structure solution was obtained using Direct Methods implemented in SHELXS [36] and the model refinement was performed with full matrix least squares on F^2 using SHELXL [36], with final residuals R1 = 0.037, wR2 = 0.105 for 2461 observed data with $I>2\sigma(I)$, and R1 = 0.046, wR2 = 0.111 for all data. The data completeness allowed for a qualitative decision of the chirality, however because only low weight atoms are present, the Flack parameter has a relatively large standard deviation, being 0.04(19). The crystal packing is stabilized by an intermolecular hydrogen bond of type N1–H1…O1^i, building a linear chain though (100). Hydrogen bond geometry is given in Table 6. The programs ORTEP-3 [20], SHELXS/SHELXL [36] were used within WinGX [37] software package.

Crystallographic data Information

Crystallographic data of compound **5b** (excluding structure factors) have been deposited with the Cambridge Crystallographic Data Centre as supplementary publication number CCDC 940524. Copies of the data can be obtained, free of charge, on application to CCDC, 12 Union Road, Cambridge CB2 1EZ, UK [fax: C44 1223 336033 or e-mail: deposit@ccdc.cam.ac.uk].

Solubility Assay

The solubility assay was performed considering the absorptivity of compounds in ultraviolet spectroscopy as described by Schneider and coworkers [38]. The assay wavelength was determined by the λ max characteristic of each compound.

Saturated aqueous solutions were prepared (0.01 mg/mL) and were kept under stirring for 2 hours at 37°C. The supernatant was filtered in 0,45 μm filters and transferred to a quartz cuvette (10 mm) to spectra acquisition.

Solubility was determined by linear regression using as graph plots, solutions prepared by dilutions of the original solution in methanol. The data were obtained in triplicates and the mean values were used to the graph plots. The correlation coefficient (R^2) values were between 0.9972 and 0.9999.

In Vitro Antiproliferative Assay

Compounds (0.009–5 μg/mL) were tested for cytotoxic activity against selected cancer cell lines: SF-295 (glioblastoma), HCT-8 (colon), MDAMB-435 (melanoma), HL60 (leukemia), PC3M (prostate cancer), OVCAR-8 (ovaries adenocarcinoma) and NCI-H258M (pulmonary bronchio-alveolar carcinoma). All cell lines were kindly obtained from the National Cancer Institute (Bethesda, MD, USA).Tumor cell proliferation was quantified through the ability of living cells to reduce the yellow dye 3-(4,5-dimethyl-2-thiazolyl)-2,5-diphenyl-*2H*-tetrazolium bromide (MTT, Sigma Aldrich)) to a purple formazan product and absorbance was measured at 595 nm (DTX-880, Beckman Coulter) [21].

Tubulin Polymerization Assay

The tubulin polymerization assay was performed by CEREP®, as described by Bonne and co-workers [39].

Hollow Fiber Assay

A total of 26 female BALB/c nude (nu/nu) mice aging 6–8 weeks were obtained from the animal facilities of State University of São Paulo (USP), Faculty of Medicine, São Paulo (SP), Brazil. They were kept in well-ventilated and sterile cages (Alesco, São Paulo) under standard conditions of light (12 h with alternative day and night cycles) and temperature (22±1°C) and were housed with access to commercial sterile rodent stock diet (Nutrilabor, São Paulo, Brazil) and water *ad libitum*. As previously mentioned procedures are in accordance with guidelines for the welfare of animals in experimental neoplasia [40] and with national and international standard on the care and use of experimental laboratory animals [41] and were approved by the local Ethical Committee on Animal Research (Process No. 102/2007).

Cell Culture

Cell culture of SF-295 (glioblastoma) and HCT-116 (colon carcinoma) was performed in RPMI 1640 medium supplemented with 10% fetal bovine serum, 2 mM glutamine, at 37°C with 5% CO_2.

HF Preparation, Surgery Deployment and Determination of the Antiproliferative Capacity

Polyvinylidene fluoride (PVDF) HFs with a 1-mm internal diameter and a molecular weight cutoff point of 500 kDa were used (Spectrum Laboratories, Houston, TX). The fibers were cut

Table 6. Intermolecular hydrogen bond geometry.

D—H…A	D—H (Å)	H…A (Å)	D…A (Å)	D—H…A (°)	Symmetry operation
N1-H1…O1^i	0.84(3)	2.12(3)	2.949(2)	170(2)	i) ½+x, 1-y, z

doi:10.1371/journal.pone.0085380.t006

into pieces 12–15 cm long, washed 2× with sterile distilled water and kept in sterile conditions.

Before use, under sterile conditions, the fibers were incubated in complete RPMI with 20% fetal bovine serum (FBS) overnight (packaging time). Cell viability was assessed by trypan blue exclusion assay. Then, a cell suspension of 7.0×10^6 cell/mL at 4°C was injected into the fiber, with the ends thereof immediately heat-sealed. The fibers were cut into 2 cm each, transferred to petri plates and incubated in complete RPMI medium for 24 h prior to implantation in mice. Each cell was injected into one fiber of a different color (HCT-116, yellow fibers; SF-295, blue fibers).

Mice were anaesthetized with ketamine (90 mg/kg) - xylazine (4.5 mg/kg) (Sigma Aldrich). Groups were divided into: a) Negative control (DMSO 5%, n = 6); b) Positive control (5-Flouoruracil, 5-FU, 25 mg/kg/day, n = 7) (Sigma Aldrich); c) LASSBio-1586 (**5b**; 25 mg/kg/day, n = 7); d) LASSBio-1586 (**5b**; 50 mg/kg/day, n = 6). A small incision in the neck was incised to permit subcutaneous (s.c.) implantation of the fibers in the dorsal part of the animal. Each animal received 2 fibers at s.c. site. All incisions were sealed with a surgical stapler. The test compounds were administered intraperitoneally during 4 consecutive days. On day 5, fibers were removed to quantify the antiproliferative capacity as described above.

In Vivo Antiproliferative Assay

Tumor cell proliferation was quantified through the ability of living cells to reduce the yellow dye 3-(4,5-dimethyl-2-thiazolyl)-2,5-diphenyl-*2H*-tetrazolium bromide (MTT, Sigma Aldrich) to a purple formazan product [21]. For this purpose, the fibers removed from animals were incubated with MTT 1 mg/mL in 6-well plates during 4 h at 37°C, 5% CO_2 and 95% humidity. The MTT solution was aspirated; fibers were washed with saline solution containing protamine sulphate 2.5% and incubated in protamine solution overnight at 4°C. Fibers were transferred to 24 well plates, cut into 2 or 3 pieces and put to dry. The formazan was dissolved in 500 mL of DMSO, aliquots (150 uL) were transferred to 96 well plates and absorbance was measured at 595 nm (DTX-880, Beckman Coulter).

Statistical Analysis

In order to determine differences between groups, data (mean ± S.E.M) were compared by one-way analysis of variance (ANOVA) followed by Student Newman-Keuls test ($P<0.05$).

Molecular Modeling

Compounds were constructed and submitted to a conformational analysis by molecular mechanics (MMFF method) with the Spartan 8.0 software (Wavefunction Inc.; Licence number: DQAIR/HASPUSB). The most stable conformer of each structure was reoptimized with the AM1 semiempirical molecular orbital method [42] and saved as mol2 files for docking studies into the colchicine binding site of the β-tubulin crystallographic structure available in the Protein Data Bank with code 1sa0. This structure was chosen because of the β-tubulin conformation induced by the co-crystallized colchicine, which prevents curved β-tubulin from adopting a straight structure, inhibiting assembly. Docking studies were implemented with the GOLD 5.0.1 program (CCDC), which employs a genetic algorithm for docking flexible ligands into protein binding sites and ranks the resulting poses according to their scores determined by available scoring functions. Hydrogen atoms were added to the protein structure according to the tautomeric and ionized states inferred by the program. The colchicine structure was removed for the docking studies, which were performed with the ChemScore scoring function, which contains specific energy terms for hydrogen bonding and lipophilic interactions [43,44]. The data and poses were analyzed on Pymol program. Licences numbers: Pymol (8588); Gold (G/414/2006).

Supporting Information

Figure S1 β-tubulin polymerization assay performed by CEREP.
(TIF)

Figure S2 The pose of CA-4 Z-isomer (A) and E-isomer (B) at colchicine binding site of β-tubulin protein (PDB:1sa0).
(TIF)

Figure S3 Scatter plots (score x cLogP and score x molecular weight).
(TIF)

Figure S4 Compounds 5i (A), 5k (B), 5n (C) and 11 (D) poses at colchicine binding site of β-tubulin protein (PDB:1sa0).
(TIF)

Acknowledgments

The authors thank Karine Ferreira Campos and Irwin Valentim da Silva for technical support.

Author Contributions

Conceived and designed the experiments: LML JRS RC CP EJB. Performed the experiments: DNA BCC DPB PMPF RPC CMLM CMRS. Analyzed the data: LML EJB CMRS JRS RC CP DNA. Contributed reagents/materials/analysis tools: LML EJB JRS RC CP. Wrote the paper: LML DNA CP. Design conception: LML EJB. Synthesis: DNA LML EJB. Molecular modelling: DNA CMRS. Experimental design: LML EJB RC CP BCC. In vivo experiments: CP RC PMPF CMLM DPB. Raios-X: JRS RPC.

References

1. Nogales E (2000) Structural insights into microtubule function. Annual Review of Biochemistry 69: 277–302.
2. Desai A, Mitchison TJ (1997) Microtubule polymerization dynamics. Annual Review of Cell and Development Biology 13: 83–117.
3. Singh P, Rathinasamy K, Mohan R, Panda D (2008) Microtubule Assembly Dynamics: An attractive target for anticancer drugs. IUBMB Life 60: 368–375.
4. Jordan MA, Wilson L (2004) Microtubule as a target for anticancer drugs. Nature Reviews: Cancer 4: 253–263.
5. Snyder JP, Nettles JH, Cornett B, Downing KH, Nogales E (2001) The binding conformation of taxol in β-tubulin: a model based on electron crystallographic density. Proceeding of the National Academy of Sciences of United States of America 98: 5312–5316.
6. Prisen VE, Honess DJ, Stratford MR, Wilson J, Tozer GM (2002) The vascular response of tumor and normal tissues in the rat to the vascular targeting agent, combretastatin A-4 phosphate, at clinically relevant dose. Int. J. Oncology 21: 717–726.
7. Fürst R, Zupkó I, Beréyi A, Ecker GF, Rinner U (2009) Synthesis and antitumor evaluation of cyclopropyl-containing combretastatin analogs. Bioorganic & Medicinal Chemistry Letters 19: 6948–6951.
8. Tron GC, Pirali T, Sorba G, Francesca P, Busacca S, et al. (2006) Medicinal Chemistry of combretastatin A-4: Present and future directions. Journal of Medicinal Chemistry 49: 3033–3044.
9. Shan Y, Zhang J, Liu Z, Wang M, Dong Y (2011) Developments of combretastatin A-4 derivatives as anticancer agents. Current Medicinal Chemistry 18: 523–538.
10. Lee L, Robb LM, Lee M, Davis R, Mackay H, et al. (2010) Design, synthesis and biological evaluations of 2,5-diaryl-2,3-dihydro-1,3,4-oxadiazoline analogs of combretastatin-A4. Journal of Medicinal Chemistry 53: 325–334.

11. Combes S, Barbier P, Douillar S, McLeer-Florin A, Bourgarel-Rey V, et al. (2011) Synthesis and biological evaluation of 4-arylcoumarin analogues of combretastains. Part 2. Journal of Medicinal Chemistry 54: 3153–3162.
12. Ravelli RB, Gigant B, Curmi PA, Jourdain I, Lachkar S, et al. (2004) Insight into tubulin regulation from a complex with colchicines and stathmin-like domain. Nature 428: 198–202.
13. Bai R, Covell DG, Pei XF, Ewell JB, Nguyen NY, et al. (2000) Mapping the Binding site of colchinoids on β-tubulin. The Journal of Biological Chemistry 275: 40443–40452.
14. Ducki S, Forrest R, Hadfield JA, Kendall A, Lawrence NJ, et al. (1998) Potent antimitotic and cell growth inhibitory properties of substituted chalcones. Bioorganic & Medicinal Chemistry Letters 8: 1051–1056.
15. Ducki S, Rennison D, Woo M, Kendall A, Chabert JFD, et al. (2009) Combretastatin-like chalcones as inhibitors of microtubule polymerization. Part-1: Synthesis and biological evaluation of antivascular activity. Bioorganic & Medicinal Chemistry 17: 7698–7710.
16. Ducki S, Mackenzie G, Greedy B, Armitage S, Charbert JFD, et al. (2009) Combretastatin-like chalcones as inhibitors of microtubule polymerization. Part-2: structure-based of alpha-aryl chalcones. Bioorganic & Medicinal Chemistry 17: 7711–7722.
17. Wermuth GC (2008) The Practice of Medicinal Chemistry, Thirth edition. Academic Press. pp. 448–452.
18. Dorléans A, Gigant B, Ravelli RBG, Mailliet P, Mikol V, et al. (2009) Variations in the colchicine-binding domain provide insight into the structural switch of tubulin. Proceeding of the National Academy of Sciences of United States of America 33: 13775–13779.
19. Lima PC, Lima LM, da Silva KCM, Léda PHO, Miranda ALP, et al. (2000) Synthesis and analgesic activity of novel N-acylhydrazones and isosters, derived from natural safrole. European Journal of Medicinal Chemisty 35: 187–203.
20. Farrugia LJ (1997) Ortep-3 for windows – a variation of Ortep III with a graphical user interface. Journal of Applied Crystallography 30: 565–566.
21. Mosman T (1983) Rapid Colorimetric Assay for cellular growth and survival: application to proliferation and cytotoxicity assays. Journal of Immunological Methods 65: 55–63.
22. Jin L, Chen J, Song B, Chen Z, Yang S, et al. (2006) Synthesis, structure, and bioactivity of N′-substituted benzylidene-3,4,5-trimethoxybenzohydrazide and 3-acetyl-2-substituted phenyl-5-(3,4,5-trimethoxyphenyl)-2,3-dihydro-1,3,4-oxadiazole derivatives. Bioorganic and Medicinal Chemistry Letters 16: 5036–5040.
23. Kümmerle AE, Raimundo JM, Leal CM, da Silva GS, Balliano TL, et al.. (2009) Studies towards the identification of putative bioactive conformation of potent vasodilatador arylidene N-acylhydrazone derivatives. European Journal of Medicinal Chemistry 44: 4004–4009.
24. Yogeeswari P, Sriram D, Thirumurugan R, Raghavendran JV, Sudhan K, et al. (2005) Discovery of N- (2,6- dimethylphenyl)- substituted semicarbazones as anticonvulsants: hybrid pharmacophore-based design. Journal of Medicinal Chemistry 48: 6202–6211.
25. Hollingshed MG, Alley MC, Camalier RF, Abbott BJ, Mayo JG, et al. (1995) *In vivo* cultivation of tumor cells in hollow fibers. Life Sciences 57: 131–141.
26. Hall LA, Krauthauser CM, Wexler RS, Hollingshed MG, Slee AM, et al. (2000) The Hollow Fiber assay: Continued characterization with novel approaches. Anticancer Research 20: 903–911.
27. Sadar MD, Akopian VA, Beraldi E (2002) Characterization of a new in vivo hollow fiber model for the study of progression of prostate cancer to androgen independence. Molecular Cancer Therapies1: 629–637.
28. Suggitt M, Swaine DJ, Petit GR, Bibby MC (2004) Characterization of the hollow fiber assay for the determination of microtubule disruption in vivo. Clinical Cancer Research 10: 6677–6685.
29. Cao X, Wang Y, Li S, Chena C, Ke S (2011) Synthesis and biological activity of a series of novel N-substituted lactams derived from natural gallic acid. Journal of Chinese Chemical Society 58: 35–40
30. Mazzone G, Bonina F, Formica F. (1978) Su alcuni aroilidrazoni di alogenobenzaldeidi e 2,5-diarial-1,3,4-ossadiazoli alogeno-sostituiti. Il Farmaco – Ed. Scientifica 33: 963–971.
31. Borchhardt DM, Mascarello A, Chiaradia LD, Nunes RJ, Oliva G, et al. (2010) Biochemical evaluation of a series of synthetic chalcone and hydrazide derivatives as novel inhibitors of cruzain from Trypanossoma cruzi. Journal of Brazilian Chemical Society 21: 142–150.
32. Mazzone G, Reina R (1991) 3,4,5-trimetossibenzoil idrazidi ad attività IMAO. Bolletino delle Sedute della academia gionia di scienze naturali in Catania 8: 689–702.
33. Horwitz JP, Grakauskas VA (1954) 1,5-disubstituted tetrazoles from1-acetyl-2 -para-substituted benzoyl hydrazines and p-nitrobenzene diazonium chloride. Journalof Organic Chemistry 19: 194–201, 1954.
34. Andrade MM, Barros MT (2010) Fast synthesis of N-acylhydrazones employing a microwave assisted neat protocol. Journal of Combinatorial Chemistry 12: 245–247
35. Mack CH, McGregor HH, Hobart SR (1969) Synthesis of some phenyl N-aroyl carbamates. Journal of Engineering data 14: 258–261.
36. Sheldrick GM (2008) A Short history of SHELX. Acta Crystallographica Section A 64: 112–122.
37. Farrugia LJ (1999) WinGX suite for small-molecule single-crystal crystallography. Journal of Applied Crystallography 32: 837–828.
38. Schneider P, Hosseiny SS, Szczotka M, Jordan V, Shlitter K (2009) Rapid solubility determination of the triterpenes oleanoic acid and ursolic acid by UV-spectroscopy in different solvents. Phytochemistry Letters 2: 85–87.
39. Bonne D, Heusèle C, Simon C, Pantaloni D (1985) 4′,6-Diamino-2-phenylindole, a fluorescent probe for tubulin and microtubules. The Journal of Biological Chemistry 260: 2819–2825.
40. United Kingdom Co-ordinating Committee on Cancer Research (UKCCCR) (1998) Guidelines for the welfare of animals in experimental neoplasia (second edition). British Journal of Cancer 77: 1–10.
41. Directive 86/609/EEC. Council Directive of 24 November 1986 on the approximation of laws, regulations and administrative provisions of the Member States regarding the protection of animals used for experimental and other scientific purposes.
42. Dewar MJS, Zoebisch EG, Healy EF, Stewart JJP (1998) Development and use of quantum mechanical molecular models. 76. AM1: A new general purpose quantum mechanical molecular model. Journal of American Chemical Society 107: 3902–3909.
43. Eldridge MD, Murray CW, Auton TR, Paolini GV, Mee RP (1997) Empirical scoring functions: I. the development of a fast empirical scoring function to estimate the binding affinity of ligands in receptor complexes. Journal of Computer-Aided Molecular Design 11: 425–445.
44. Baxter CA, Murray CW, Clark CE, Westhead DR, Eldridge MD (1998) Flexible docking using tabu search and an empirical estimate of binding affinity Proteins: Structure, Function and Bioinformatics 33: 367–382.